MARINE RESEARCH

BUREAU OF COMMERCIAL FISHERIES

25

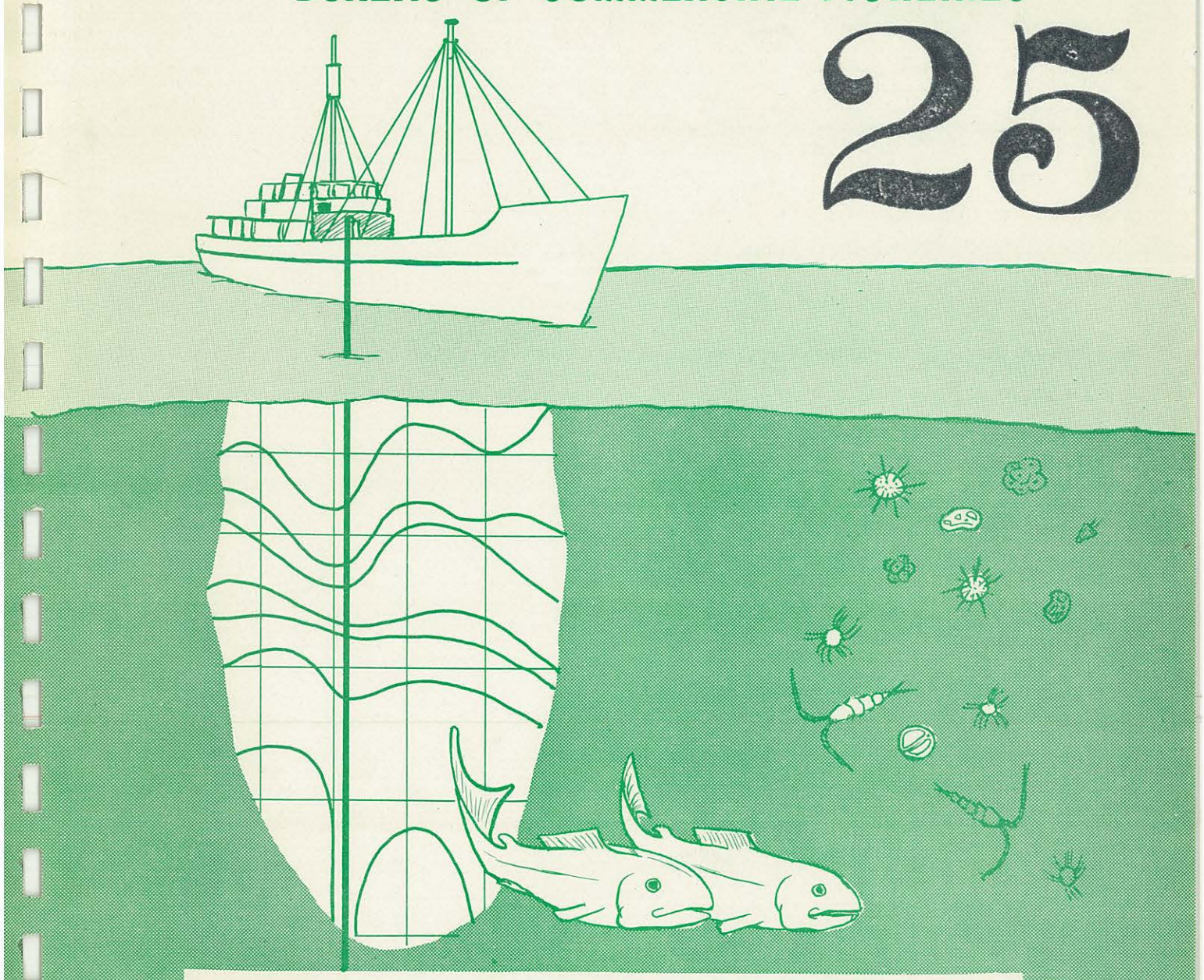

OCEAN CIRCULATION IN THE VICINITY OF THE ALEUTIAN ISLANDS, 1957

by Richard J. Callaway

BIOLOGICAL LABORATORY SEATTLE, WASHINGTON

Check for Dup before filing

October 10, 1960

OCEAN CIRCULATION IN THE VICINITY OF THE ALEUTIAN ISLANDS, 1957

by

Richard J. Callaway

Oceanographer

Bureau of Commercial Fisheries
Biological Laboratory
Seattle, Washington

CONTENTS

TABLES

FIGURES

ABSTRACT

Data collected by Canadian, Japanese and United States vessels during the summer of 1957 are utilized to describe the physical oceanography of the Aleutian Islands region.

A brief review of the bottom topography, tidal currents and climatology of the region is given.

Vertical and lateral sections of temperature, salinity and sigma-t are shown and their significance discussed.

OCEAN CIRCULATION IN THE VICINITY OF THE ALEUTIAN ISLANDS, 1957

by

Richard J. Callaway
Oceanographer
Bureau of Commercial Fisheries
Biological Laboratory

INTRODUCTION

As part of the International North Pacific Fisheries Commission (INPFC) program of research on the high-seas distribution and abundance of salmon, the Bureau of Commercial Fisheries initiated, in 1955, the collection of oceanographic data in the Bering Sea - North Pacific region.

Since that time, spring and summer surveys have been made each year. The 1955, 1956 cruises were conducted by the University of Washington under contract to the Bureau. The data reports for those years have been compiled by Favorite and Love (1957), and Love (1957, 1959).

Since 1957 the data have been collected and processed by USFWS personnel (Favorite and Pedersen, 1959a, b.) This report is based on the oceanographic cruises of Canadian, Japanese, and United States vessels during the period July 19-August 31, 1957. Most of the measurements were made from the USFWS vessels Attu, Paragon, and Pioneer.

Dissolved oxygen and inorganic phosphate measurements were made by some of the vessels; however, the observations were too few to permit separate analysis of these parameters.

Description of the Region

The terms "region" or "area" encompass 45° - 56°N. latitude, 150°W. - 175°E. longitude. The terms "Aleutian Islands" and "Aleutian Chain" are used to include the arc of islands from Unimak to Attu. "Aleutian ridge" refers to the submerged sections between the islands. In citing positions the terms "latitude" and "longitude" will usually be omitted.

The Coast Pilot for Alaska (U. S. Coast and Geodetic Survey, 1955) provides such information as local weather conditions and tidal currents, in the vicinity of the Alaskan Peninsula and Aleutian Islands. Fleming (1955) has reviewed the general features of the area and has included an extensive bibliography.

Figure 1 gives the names of the principal islands and passes in the Aleutian chain. The 100, 1000, and 5500 meter isobaths are also shown.

In the Bristol Bay region, there is a broad, shallow shelf which extends westward of the Pribilof Islands. The 100-meter contour is not drawn in the Aleutian region since it nearly coincides with the 1,000-meter contour.

The Aleutian Islands rise precipitously from depths of greater than 7,000 meters in the Aleutian Trench and greater than 3,500 meters in the Bering Sea. As may be seen, the 1,000-meter contour is quite close to the islands with the exception that at the 180° meridian it extends into Bering Sea enclosing Bowers Bank, where depths of less than 130 meters are reported. It is noted that on some charts the name "Bowers Bank" refers only to a shallow bank (less than 100 fathoms) situated at about 54 25'N., 179°45'E.

Only Amchitka Pass (179°W.) is deep enough to allow exchange of waters at depths exceeding 1,000 meters.

Tidal Currents

Tidal currents in the region are, according to the Coast Pilot (op. cit.), ". . . highly complex, making generalizations impossible . . .. All passages in the Aleutian Islands have strong currents. In the narrow Akun Strait, the current is reported to reach a velocity of 12 knots."

In southeastern Bering Sea, north of Unimak Island, Hebard (1959) observed the tidal currents in June, 1957, by means of an Ekman current meter, for two offshore and two inshore stations. Measurements were made at the surface, top and bottom of the thermocline and the bottom. The flow of the average current was counter-clockwise. At the offshore (56°56'N., 164°30'W; 57°40'N, 161°53'W.) stations dextrally rotating tidal currents occurred with a maximum of between 1.0 and 1.5 knots flowing parallel to the coast. The inshore (56°37'N., 160°59'W; 55°40'N., 163°24'W.) stations exhibited rotary tidal currents, with varying degree of rotation; the maximum currents were between 0.8 and 1.7 knots parallel to the coast.

Weather

Quoting further from the Coast Pilot: "The weather of the Aleutians is characterized by persistently overcast skies, high winds, and violent storms. No other area in the world is recognized as having worse weather in general than that which the Aleutian Islands experience."

Winds in the Aleutian region are generally influenced by the Aleutian Low which fills in during May and gradually loses its identity through June and July. By August the Low appears in the north Bering Sea, becoming stronger with the winter months.

Winds in May have a northwesterly or westerly component. During the summer months the previaling winds are from the south or southwest.

Evaporation

Jacobs (1951) has prepared mean charts which show evaporation in the area as being 0-0.05 cm/day, for the period June-August. Precipitation minus evaporation is shown as about 15-20 cm. for the season.

Dilution

Fresh water is also added to the region by runoff and ice melt. In Bering Sea, the Yukon and Kuskokwim Rivers, and in Bristol Bay, the Ugashik, Egegik, Naknek, Kvichak and Nushagak Rivers contribute heavily to the runoff. On the south central coast of Alaska, the Copper and Susitna Rivers supply much of the fresh water runoff. In addition, there are numerous streams and small rivers which add to the net dilution of Bering Sea and Subarctic[1/] waters.

Ice breakup in the Nushagak, Kuskokwim and Susitna Rivers begins, on the average, early in May.

1/ The term "Subarctic waters" is used in this paper to describe that portion of the North Pacific Ocean where the salinity minimum is at the surface. "Subpolar" will include Bering Sea, Bristol Bay and Subarctic North Pacific waters.

Reports Utilizing 1957 data

The location of the stations used is shown in figure 2.

Not all of the data from the aforementioned cruises were utilized. Some stations were outside the area under investigation. Other stations were occupied before or after the period of July 19 - August 31.

Dodimead (1958) has discussed the 1957 horizontal distribution of properties in the Gulf of Alaska. He has also described the vertical section based upon Oshawa stations 16 and 28-37 (see fig. 2).

Kitano (1958) has presented horizontal and vertical sections based on the 1957 cruise of the Tenyo Maru and a preliminary report on oceanographic conditions observed from the MV Attu, Paragon and Pioneer has been presented by Favorite in INPFC (1959). Aron (1959) has utilized 1957 Brown Bear data in a paper dealing with midwater trawling in the North Pacific and Bering Sea.

SELECTION OF TIME PERIOD

Figure 3 is taken from Robinson (1957). The curve showing surface temperature indicates that the rate of change of temperature from July 20 to September 1 is negligible. Fleming (1955) has presented a time-series cycle of temperature representing the degree square 52° - 53°N, 178°-179°E. The surface temperature peak is shown as about August 10.

The temperature-salinity (T-S) diagrams for several locations have been presented in INPFC (1959), and are reproduced here as figures 4 to 6. It is immediately apparent from the diagrams that the period of summer heating of the surface waters has continued into late August. The surface waters have generally become more dilute as the season progressed.

The T-S diagrams, then, show that for the upper water column the vertical and horizontal sections of temperature, salinity, and sigma-t will include seasonal effects. Ideally, one would like to be able to represent the temperature field when the rate of change of temperature is nearly zero for the time period covered.

Changes in the water column below about 300 meters will be due primarily to advection and not to the direct influence of external processes. This is apparent from the temperature cycle shown in figure 3 which reveals a considerable lag in the diffusion of heat from the surface to deeper water.

In contouring the various fields it is assumed that the oceanographic stations were occupied synoptically. In lieu of a synoptic survey it is advisable to select a time period when oceanic conditions are as near to being stationary as possible. With regard to temperature, the period July 19 - August 30 provides the least rate of change. For this reason some earlier data collected by USFWS vessels and the Japanese vessel Oshoro Maru were not used.

Averaging of Data

Some stations were occupied several times. Where this occurred interpolated data at standard depths were averaged,[2/] the resulting values being used in the sections. In some instances, where the depth of the Nansen

---

2/ Temperature and salinity average values were used to obtain an average sigma-t.

bottle casts reached different depths, only the data in the upper 150-300 meters were averaged.

To remove the undetermined effects of interval wave activity, each station should be occupied more than once. If data from only a few stations are averaged, the stations occupied only once will, presumably, assume more importance than they should. Taking average values of, for example, surface temperature at 53°N., 175°E., (fig. 4) puts the temperature in the middle of the upward slope of the time series curve (fig. 3). If the last station occupied at a given location were used, further bias would be provided because adjacent, single stations may have been occupied at different times on the cycle.

SOURCES OF DATA

The sources of data utilized, details of salinity analytical methods and treatment of data will be found in the references cited in table 1.

CURRENTS

As an introduction to this section a brief discussion of the method of determining geostrophic currents is presented. The geostrophic equation is a familiar one in meteorology and oceanography. The assumption is made that the magnitude of inertial and frictional forces is much less than the magnitude of the horizontal pressure gradient force and the apparent force due to the earth's rotation (Coriolis force). Geostrophic velocities and transports are calculated from the balance of the latter two forces.

Table 1.--Sources of data

Vessel	Abbreviation (Used in vertical sections)	Period (1957)	Stations used	Authority
Attu	A	19 Jul.-23 Aug.	14-34	Favorite and Pedersen (1959a)
Paragon	Pn	21 Jul.-31 Aug.	1-20	" " " "
Pioneer	P	21 Jul.-31 Aug.	12-30	" " " "
Brown Bear	B	9-29 Aug.; 30 Jul.-2 Aug.	1/1-23; 35-37	R. H. Fleming and Staff (1958)
Horizon		27 Jul.-8 Aug.	6-10	Scripps Institution of Oceanography 2/
Oshawa		30 Jul.-11 Aug.	14-37	Pacific Oceanographic Groups (1957)
Tenyo Maru	T	19-30 Jul.	14-42	Hokkaido Regional Fisheries Laboratory (1958)

1/ Brown Bear station 16 was omitted in the data report. Prefixes to Brown Bear station numbers omitted here and in figure 1.

2/ Manuscript of physical and chemical data collected on the Mukluk expedition by Scripps Institution of Oceanography.

Charts of the anomaly of geopotential topography show geostrophic current directions in the form of isolines of dynamic height. The velocities are inversely proportional to the spacing of the isolines, in a narrow latitude range. Dynamic height calculations are made for each oceanographic station by integration of the anomaly of specific volume (the difference of the observed volume per unit mass from a unit mass of water at 0°C., 35°/oo salinity and at the observed pressure) from a reference level to the desired depth. It is assumed that motion at the reference level is negligible.

The surface current pattern relative to the 300 decibar (approximately 300 meters) level is shown in figure 7. The choice of the 300 db. level is not to imply that this is a level of no motion, but was made because not enough stations could be used if a deeper level were selected. A shallower level would be subject to short term external influences. As will be shown in a discussion of the vertical sigma-t sections near the islands there is a large pressure gradient at 300 meters and deeper, which implies considerable motion at the reference level. Nevertheless, it is felt that the current directions as shown in the figure are representative. The magnitude of the mean flow (i.e., the spacing of the contours) cannot be considered a very close approximation.

It is apparent that the currents are related to bottom topography. A region bounded by 0.475 dynamic meters lies over the Aleutian Trench. The current flowing east, north of Attu and Kiska Islands, is deflected north by Bowers Bank. The currents north and south of the Aleutian Islands follow the 1000-meter isobaths. In the vicinity of Unalaska

Island, the currents have a northward component. The current charts of Barnes and Thompson (1938) and Goodman et al. (1942), show northward flow between the 100 and 1000-meter isobaths that lie west of the Pribilof Islands.

The westward flow along the south of the islands is due primarily to surface accumulation of fresh water along the Alaskan Peninsula. This flow would be analagous to the estuarine-type circulation proposed by Tully and Barber (1960).

The above-mentioned relation between surface flow and the Aleutian Trench is only incidental to the current pattern. If the Aleutian Trench does influence circulation in the region this influence is probably confined to the deep circulation.

The station spacing in the vicinity of Bowers Bank does not allow conjecture on the possibility of a leeside wave. Sverdrup et al. (1942) have pointed out that the expected deflections due to bottom topography may be masked by synoptic surveys.

GEOPOTENTIAL HEIGHTS

In two water columns with the same temperature (or salinity) distribution, the less saline (or warmer) column will have a higher steric level. The integrated effect of temperature and salinity on the potential energy distribution in a water column with reference to an assumed level surface is shown by charts of geopotential anomaly. In order to determine the relative influence of either temperature or salinity on steric levels, calculations must be made of thermal and haline departures, since the

steric departure from a reference sea level is nearly equal to the algebraic sum of thermal and haline departures 3/

Figure 8 shows the geopotential anomaly of the isobaric surfaces relative to the 1000 db. level along 175°E. longitude. The range of the isobaric levels is indicated by vertical lines. If one considers the surface isobaric level from 50° - 51°30' N. and from 53° - 54°30' N. the average dynamic level north of the island is higher than to the south, approximately 1.065 versus 1.010 dyn. m.

The average dynamic height at 51°30' N. is 0.064 dyn. m. greater than at 53°N. Assuming similar atmospheric pressure conditions on both sides of the island, there is inferred a difference in sea level of about 6 geometric cm., the water column south of the islands being higher than to the north. Whether or not this condition obtains closer inshore can only be established through precise levelling.

Figure 9 shows the surfaces relative to 800 db. The large variations in the vicinity of Amchitka Pass have been interpreted in figure 7 as isolated cells.

3/ Patullo, et al., (1955) define the thermal(Z_t) and haline (Z_s) departures as follows:

$$Z_t = g^{-1} \int_{p_a}^{p_o} \frac{\partial \alpha}{\partial T} \Delta T dp$$

$$Z_s = g^{-1} \int_{p_a}^{p_o} \frac{\partial \alpha}{\partial s} \Delta S dp ,$$

where

α = specific volume anomaly,
T,S = temperature, salinity, respectively,
g = acceleration due to gravity,

and the integration is from atmospheric pressure to a pressure where all seasonal effects are assumed to vanish.

The meridional isobaric surfaces along 175°W. are shown in figure 10. The situation adjacent to the islands is the reverse of that along 175°E. The dynamic level at 52°30' N. is 10.9 dyn. cm. greater than at 51°30' N.

As in the vertical sections of salinity and sigma-t, the geopotential sections bring out the fact that dilution in Bering Sea decreases westward, and that the Aleutian chain acts as a barrier separating the saline[4] waters of the Pacific Ocean from the Bering Sea. The effect of cooler temperature in reducing steric levels increases westward. This is shown along 175°E. longitude. At 51°30'N. and 53°N., the salinity distribution in the water columns is nearly the same but the steric level south of the Aleutian ridge is greater than north of it.

LATERAL DISTRIBUTION OF SIGMA-T

Charts showing the variations with depth of a particular value of sigma-t provide a three-dimensional view of subsurface circulation, in that currents tend to be parallel to isolines of sigma-t. Lateral mixing of greatest intensity takes place in the surface of constant potential density[5] and the flow patterns are more stable and simpler than those on a horizontal surface (Montgomery, 1938).

4/ The terms "saline" and "fresh" will be used to mean "relatively saline" and "relatively fresh".

5/ Sigma-t = σ_t = 10^3(specific gravity -1). A sigma-t surface is one of approximately constant potential density in the upper 1000 meters. Isentropic analysis refers to changes of properties on surfaces of constant entropy or sigma-t surfaces.

Near the islands and in the island passes, non-isentropic mixing occurs and the principles of isentropic analysis do not apply. In the use of isentropic analysis, one assumes that the effects of viscosity and vertical diffusion are negligible.

The reader should keep in mind that looking downstream the sigma-t surface deepens to the observer's right (in the Northern Hemisphere).

Figures 11 and 12 show the depth of, and salinity on, the 26.0 sigma-t surface. Immediately south of the islands at about 165°W., there is a tongue (100 meters) that flows along the south of the islands becoming shallower to the west.

There is a shallow (less than 25 meter) layer surrounding the islands from about 171°W. to 170°E. The sigma-t curves indicate a movement of water through Amchitka Pass into the Bering Sea, although this is a region of non-isentropic mixing.

In the Bering Sea, the depth of the surface decreases northward to 25 meters. The cell of greater than 50 meters at 173°W. is based on a single observation of 70 meters.

Figures 13 and 14 show the depth of, and salinity distribution on, the 26.5 sigma-t surface. This surface deepens rapidly when one approaches the islands from the south. The depth chart indicates that between 125-150 meters there is a steady motion that sweeps the entire length of the Aleutian Chain. Again, there is a ridge extending east-west bounded by the 125 meter contour. In the eastern part of the figure the ridge penetrates into the upper 100 meters.

Several anticyclonic cells are present near the islands, and a single large cyclonic cell is situated to the east.

In the Bering Sea, the depth of the surface decreases to the northwest.

The salinity distribution on this surface implies a region of discontinuity at about 51°N., 172°W. This discontinuity is present also on the 26.0 sigma-t surface, but farther to the west. The depth chart for the 26.5 sigma-t surface shows an intrusion of water from the south that could account for this discontinuity.

Figure 15 shows the depth of the 27.0 sigma-t surface. The salinity variation on this surface was too slight to permit contouring. Once again the sigma-t isolines are continuous along the Aleutian Chain. Only on the 26.0 sigma-t surface was there any indication of movement into Bering Sea. No doubt there is more exchange than is here indicated, but the stations in and near the passes are not spaced closely enough to settle this question.

HORIZONTAL DISTRIBUTION OF TEMPERATURE

Figures 16 to 19 show the temperature distribution at 0, 100, 300, and 500 meters, respectively.

Figure 16, surface temperature, is derived from hydrographic and bathythermograph data. Due to intense vertical mixing in the upper layers, the entire island chain is shown as situated in colder[6/] waters than in the Bering Sea or Pacific Ocean. This kind of "upwelling" must be

---

6/ The terms "cold" and "warm" will be used to mean "relatively cold" and "relatively warm".

ascribed to tidal mixing rather than to wind stress associated with "classical upwelling."

The temperature distribution at 100 meters (fig. 17) differs from the surface distribution in one major respect. Here most of the Aleutian Islands are banded by warm (greater than 5.0°C.) water and the temperature decreases to the north and south. This is the result of the downward curvature of the isotherms at shallow depths near the land masses. At about 50°N., 175°W., there is a break in the less than 4.0°C. band extending east-west. As mentioned before, there is an indication that this discontinuity has been produced by advection from the south.

Figure 18 shows the temperature distribution at 300 meters. Once again the deeper waters are shown as being warm (greater than 4.0°C.) about the Aleutian Islands. The contour of 4.25° C. is drawn south of the islands east of 178°W., but it is possible, had there been more data to the north, that this isotherm could have been drawn so as to enclose the islands.

The deepest horizontal section of temperature is at 500 meters (fig. 19). The islands are shown as being surrounded in a broad band of 3.5°C. water. There are several cells drawn, based mostly on single observations.

HORIZONTAL DISTRIBUTION OF SALINITY

The horizontal distribution of salinity at 0, 10, 100, 300, and 500 meters is shown in figures 20 to 24, respectively.

The surface salinity chart (fig. 20), constructed from hydrographic and bathythermograph station shows a dilute tongue of water sweeping south of the islands. This tongue originates from runoff from the Alaska Peninsula and south coast of Alaska. Another tongue, of the same origin, is shown as moving south along 162°W. In the eastern part of the figure there is a

salinity ridge of 32.8 °/oo and a cell of less than 32.8 °/oo within this ridge. North of Unimak Island there is a salinity gradient directed into Bristol Bay. Here ice-melt and river runoff are responsible for the dilution.

The salinity distribution at 10 meters (fig. 21) is based on considerably fewer observations than at the surface. The same general features are present, however. The tongues originating near the Alaska Peninsula show fresh water moving to the south of the islands and a protrusion to the southwest. The direction of the secondary (i.e., southwest protrusion) tongue has changed and the gradients associated with both tongues have decreased in magnitude. The Bristol Bay gradient is present at 10 meters but the isohalines terminate on the northern side of the islands, while the surface isohalines were shown as connecting through the passes.

The western Bering Sea salinity distribution is essentially the same at 10 meters as at the surface. The 33.0 °/oo isohaline encloses about the same area at both depths.

The chart of salinity at 100 meters (fig. 22) includes the 33.3 °/oo isohaline to show the salinity range in the western Bering Sea. The dilute tongue south of Unimak Island is present at this depth, but the secondary tongue has disappeared. A ridge bounded by the 33.2 °/oo isohaline is present as far west as 175°W., and two elongated cells (33.4 °/oo) are shown within the ridge. In the eastern part of the ridge, another cell (33.4 °/oo) is shown. Dodimead (1958) shows this cell extending as far as 55°N., 148°W.

Figure 23 shows salinity at 300 meters. The number of stations is reduced because some casts did not reach this depth. The islands are shown as lying in a trough of less than 33.8 °/oo, the result of deepening of the isohalines near the islands.

The 500 meter section (fig. 24) shows again the east-west discontinuity of the 34.2 °/oo ridge; the 300 meter chart shows the ridge (34.0 °/oo) as discontinuous near 178° W. The islands are shown as in a trough of less than 34.0 °/oo. Salinity in the Bering Sea increases to the west, whereas at 300 meters the increase is in a northwesterly direction.

VERTICAL DISTRIBUTION OF SIGMA-T

Figure 25 sigma-t along 175° E., shows the isopleths as connecting over the submerged ridge (140 meters deep). Approaching the ridge from the south, the 26.6 isopleth sinks, then rises. The 26.4 isopleth and those above show no apparent influence of bottom features. Below 100 meters, the slope of the isopleths is greater to the south of the pass than to the north. The chart of geopotential topography (fig. 7) reflects this slope in that there is indicated a relatively swift current to the south.

Along 179° W. (fig. 26), the depth through Amchitka Pass exceeds 1000 meters. The Brown Bear stations (3, 4, 5, 7, 12, 13) indicate a deep anticyclonic motion. The slopes of the isopleths may be considerably exaggerated since data from the Tenyo Maru and Brown Bear are incorporated in this section, and since the longitude 179° W. is not that at which some of the stations lie.

The section through Atka Pass is shown in figure 27. The volume transport through this pass is, of course, quite restricted since the depth is about 25 meters. There is some exchange indicated by the connection of isopleths through this pass. Below 100 meters, the isopleths are deeper than those in Subarctic waters. Consequently, the dynamic height in Bering Sea is higher, as was mentioned before. Here, as along 179° W., the dilute tongue south of the islands is in evidence. The surface values of sigma-t

at 51°30', 51°, and 50° N. are 25.02, 25.11, and 25.19, respectively.

The depth of Amukta Pass is 380 meters (fig. 28). The 27.0 isopleth is shown as sinking into the ridge on both sides of the pass. At 51°50 N., there is an unstable[7/] layer indicated in the upper 30 meters, and in the upper 20 meters at 53°20'N. The dilute tongue in Subarctic waters is again in evidence to about 100 meters. Below 100 meters the Bering Sea isopleths are deeper than in Subarctic water.

The shallow waters of Bristol Bay connect with Subarctic water through Unimak Pass along 165° W. (fig. 29). Thompson and Van Cleve (1936) have reported recoveries of drift bottles which had presumably drifted into Bristol Bay via Unimak Pass.

7/ The expression for stability in the upper 100 meters is given by $E = (10^{-3}) \frac{d\sigma_t}{dz}$, where E is stability and z is depth.

A negative E means instability.

VERTICAL DISTRIBUTION OF SALINITY

Figures 30 to 34 show the vertical sections of salinity corresponding to the sigma-t sections. Since the isopleths of salinity and sigma-t take nearly the same course only small details would be included in a separate discussion of the salinity sections.

In the upper 100 meters, the isohalines bend toward the sea surface in the vicinity of the islands. Below 100 meters the isohalines deepen toward the submerged land masses. The isohalines in the Bering Sea are deeper than their counterparts in the Pacific Ocean, the difference in depth increasing toward the east. The 33.2 °/oo isohaline is shown as a continuous line along all longitudes except 165°W., where the 32.8 °/oo isohaline extends only into Unimak Pass.

BATHYTHERMOGRAPH SECTIONS

Bathythermograph 8/ (BT) sections are shown in figures 35 to 55. A detailed discussion of the individual BT sections will not be given here; rather, the main features will be outlined.

Stommel (1958) has pointed out that when temperature is not a monotonic function of depth, the interpretation involved in drawing isotherms through maxima and minima can be ambiguous. This is true where

---

8/ The accuracy of the BT is about ±3 meters (275 meter cast and about ±0.2°C.)

temperature inversions occur in isolated cases. It is a characteristic of Subpolar waters that a temperature minimum is found at depths ranging from 50 to 150 meters, and there is no ambiguity inferred in this widespread phenomenon.

Uda (1935) has applied the name "dichothermal" to the inversion layer. The temperature inversion below the minimum he has called "mesothermal."

In the BT sections, the dichothermal layer is bounded by the 3.0° - 4.0°C. isotherms. The minimum temperature in the layer ranges from about 1.5° C. to 3.8° C. Along 175°W., the dichothermal structure is shown as reaching its southern limit at about 50°30'N. (fig. 41). Associated with the dichothermal structure is a halocline, through which stability is maintained in the dichothermal layer.

Figures 35-40 show thermocline development along 175°E. In figures 35-36, no thermocline is present but by July 22-27 (fig. 37), the thermocline is shown at about 10-20 meters. By late July (fig. 38), the thermocline depth is 20-25 meters. In figure 39 the thermocline is shown as approaching the surface in the vicinity of the pass, but in figure 40 this feature is not present.

Figures 41-48 show the development of the thermocline along 175°W. In figures 41-42 the thermocline is as yet unformed, but figure 43 (June 30-July 5) shows that the temperature gradient between 30-60 meters has increased. In figure 44 (July 16-20) the thermocline is well developed, and by the third week in July and through August (fig. 45-48) reaches its maximum gradient in temperature across the thermocline layer and its maximum depth (30-35 Meters). In figures 45 and 48, the isothermal layer over Atka Pass indicates that tidal mixing is effective throughout the water column.

Figures 49-53 show the temperature distribution along 165° W. In figure 49 the warm (greater than 11.0°C.) dilute tongue is clearly in evidence. Warm (greater than 5.0°C.) water is shown as lying between 120-175 meters next to the submerged land mass. The effect of tidal mixing is present between 54° - 55°N., and cold (less than 2.5°C.) water of Bristol bay origin is shown between 55°30' - 56°N.

Single sections along 162°30'W. and 160°W. are shown in figures 54 and 55 respectively. In figure 54 (August 22-23), the warm water of Gulf of Alaska origin is not present as a well-defined wedge, but the 12°C. isotherm is at depths of about 15 meters. Figure 55 (July 14-19) shows the core (greater than 10°C.) as lying between 53° - 54°30'N. BT's 61-62 indicate warm (5°C.) water at depths of over 200 meters near the island.

The annual cycle of temperature (fig. 3) indicates that in February the surface waters down to 300 feet (91 meters) are isothermal, about 38.1°F. (3.4°C.). The 400-foot (122 meter) curve shows that water at this depth is about 39.1°F. (3.9°C.).

The 3.4°C. surface layer temperature is cold enough to account for most of the dichothermal layer in the Pacific Ocean; that is, presuming overturn of these waters. This process of overturn, however, is probably continuous once cooling begins.

Advection of cold Oyashio water contributes to the dichothermal structure, but overturn is the main source in the Pacific Ocean and Bering Sea as discussed below.

Sverdrup, et al. (1942, p. 732) suggest that in the Subarctic region the temperature minimum represents the depth of winter convection currents. Doe (1955) and Dodimead (1958) have also related the dichothermal layer to winter cooling and overturn. Based on data from weather station PAPA (50°N., 145°W.), Dodimead found that surface cooling in February, 1957, was less than in the previous winter. He found that in the Gulf of Alaska region the minimum temperatures were about 0.5°C. less in August, 1956, than 1957. Bennett (1959) has presented charts of the depth of minimum temperature for August, 1955, in the Gulf of Alaska. The isotherm patterns for the temperature minimum structure are closely similar to the surface geostrophic current pattern for the same period.

Graphical subtraction of BT temperature sections (not shown) reveals that, with the procession of summer, cold water advection occurs in both the Pacific Ocean and Bering Sea dichothermal structure.

SUMMARY

It has been shown by others that the Subpolar region is one of net dilution. Dilution of the surface waters by runoff continues past the time period included in this report. Surface temperature increased into late August.

It is shown that the geostrophic assumption is not a close approximation near the islands since the pressure gradient is not vanishing at depth. East of Amchitka Pass, the steric level north of the Aleutian Islands is greater than on the Pacific Ocean side. Major water exchange is through Amchitka Pass and between Attu and Kiska Islands, with the direction of flow being into Bering Sea.

In the upper 50 and 100 meters, the isotherms and isohalines, respectively, approach the surface near the islands. Below these depths they bend down. The surface temperature chart pictures the islands as lying in cold water, the result of tidal mixing in the passes and around the islands. Below 100 meters the islands are shown as lying in warm waters.

The dichothermal structure is present in the Bering Sea and Pacific Ocean. The temperatures in the dichothermal layer can be accounted for by overturn of winter-cooled surface water. Advection also contributes to the cold waters of the inversion layer. The thermocline begins to form in late June, and by the third week in July is well developed.

ACKNOWLEDGMENTS

The author is indebted to Messrs. Felix Favorite and Fred Cleaver for many suggestions. Dr. N. P. Fofonoff and Mr. Alan Dodimead of the Pacific Oceanographic Group, Nanaimo, B.C., also helpfully criticized the manuscript.

LITERATURE CITED

Aron, William

1959. Midwater trawling studies in the North Pacific. Limnology and Oceanography, Vol. 4, No. 4, p. 409-418.

Barnes, Clifford A. and T. G. Thompson

1938. Physical and chemical investigations in Bering Sea and portions of the North Pacific Ocean. University of Washington publications in Oceanography, Vol. 3, p. 35-79 and Append. p. 1-164.

Bennett, E. B.

1959. Some oceanographic features of the northeast Pacific Ocean during August, 1955. Journal Fisheries Research Board of Canada, Vol. 16, No. 5, p. 565-633.

Dodimead, A. J.

1958. Report on oceanographic investigations in the northeast Pacific Ocean during August, 1956, February, 1957 and August, 1957. MSS Report No. 20 of the Fisheries Research Board of Canada, 14 p., 35 figs.

Doe, L. A. E.

1955. Offshore waters of the Canadian Pacific Coast. Journal Fisheries Research Board of Canada, Vol. 12, No. 1, p. 1-34.

Favorite, F. and Cuthbert M. Love

1957. North Pacific Ocean and Gulf of Alaska physical and chemical data, summer and fall, 1955. University of Washington Department of Oceanography, Special Report No. 28, 88 p. 1 fig.

Favorite, Felix and Glenn Pedersen

1959a North Pacific and Bering Sea Oceanography, 1957. U.S. Fish and Wildlife Service, Special Scientific Report--Fisheries No. 292, May, 1959, 106 p.

1959b North Pacific and Bering Sea Oceanography, 1958. U.S. Fish and Wildlife Service, Special Scientific Report--Fisheries No. 312, November, 1959. 230 p.

Fleming, Richard H.

1955. Review of the oceanography of the northern Pacific. Bull. No. 2. International North Pacific Fisheries Commission 1955. 43 p.

Fleming, R. H. and Staff

1958. Physical and chemical data, North Pacific Ocean. Brown Bear Cruise 176, July-September, 1957. University of Washington Department of Oceanography Special Report No. 29. 15p. [91] p. tables.

Goodman, Joe R., J. H. Lincoln, T. G. Thompson and F A. Zeusler

1942. Physical and chemical investigations: Bering Sea, Bering Strait, Chukchi Sea during the summers of 1937 and 1938. University of Washington Publications in Oceanography, Vol. 3, No. 4, p. 105-169 and Appendix, p. 1-117.

Hebard, James F.

1959. Currents in southeastern Bering Sea and possible effects upon king crab larvae. U.S. Fish and Wildlife Service Special Scientific Report--Fisheries No. 293, 11 p.

Hokkaido Regional Fisheries Research Laboratory

1958. A preliminary data of physical oceanography obtained research vessel "Tenyo Maru" in the Bering Sea and the Aleutian waters. July-August 1957. 30 p. 1 fig. (mimeographed).

International North Pacific Fisheries Commission

1959. Report on the investigations by the United States for the International North Pacific Fisheries Commission-1958. In: International North Pacific Fisheries Commission Annual Report for the year 1958; Vancouver, Canada, p. 74-119.

Jacobs, Woodrow C.

1951. The energy exchange between sea and atmosphere and some of its consequences. Bulletin Scripps Institution of Oceanography, Vol. 6, No. 2. p. 22-122.

Kitano, Kiyomitsu

1958. Oceanographic structure of the Bering Sea and the Aleutian waters. Part I. Based on the oceanographic observations by R. V. "Tenyo Maru" of 1957. Bulletin Hokkaido Regional Fishery Research Laboratory, Vol. 19, Dec. 1958. 9 p.

Love, Cuthbert M.

1957. Physical and chemical data--Gulf of Alaska spring and summer 1956 and spring 1957. University of Washington Reports of Oceanography. Technical Report No. 56. 90 p.

1959. Physical and chemical data, North Pacific Ocean. Gulf of Alaska and Bering Sea summer of 1956. University of Washington Department of Oceanography. Special Report No. 31. 13 p. 216 p. tables, 2 figs.

Montgomery, R. B.

1938. Circulation in upper layers of southern North Atlantic deduced with use of isentropic analysis. Papers in Physical Oceanography and Meteorology, Vol. 6, No. 2, 55 p.

Pacific Oceanographic Group, Nanaimo, B.C

1957. Physical, chemical and plankton data record. North Pacific survey July 23 to August 30, 1957. Fisheries Research Board of Canada, MSS Report Series (Oceanography and Limnology) No. 4. 103 p.

Patullo, June, W. Munk, R. Revelle and Elizabeth Strong.

1955. The seasonal oscillation in sea level. Journal of Marine Research. Vol. 14, No. 1. p. 88-156. 1 chart.

Robinson, Margaret K.

1957. Sea temperature in the Gulf of Alaska and in the northeast Pacific Ocean, 1941-1952. Bulletin Scripps Institution of Oceanography, University of California Press 98 p., 1 chart.

Stommel, Henry

1958. The Gulf Stream. University of California Press and Cambridge University Press. 202 p.

Sverdrup, H. U., M. W. Johnson and R. H. Fleming.

1942. The oceans: their physics, chemistry and general biology. New York: Prentice-Hall. 1087 p.

Thompson, William F. and R. Van Cleve

1936. Life history of the Pacific halibut (2). Distribution and early life history. Reports of the International Fisheries Commission, No. 9. 184 p.

Tully, J. P. and F. G. Barber

1960. An estuarine analogy in the sub-Arctic Pacific Ocean. Journal Fisheries Research Board of Canada, Vol. 17, No. 1. p. 91-112.

Uda, M.

1935. On the distribution, formation, and movement of the dicotherm water in the northeastern sea region adjacent to Japan. Umi to Sora, Vol. 15, No. 12.

U. S. Coast and Geodetic Survey

1955. United States Coast Pilot 9: Alaska, Cape Spencer to Arctic Ocean. Government Printing Office, Washington, D.C. Sixth (1954) Edition. 673 p.

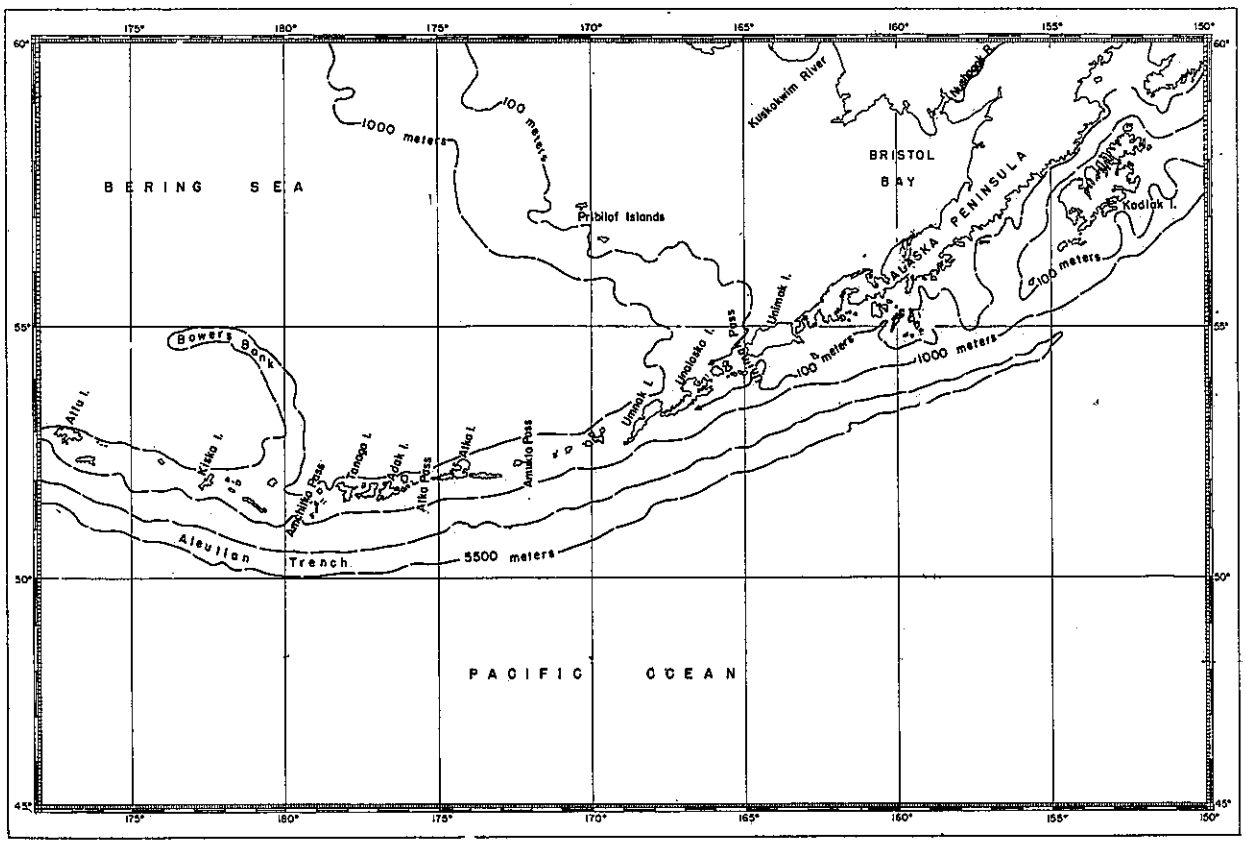

Figure 1.--Chart of the Aleutian Island area.

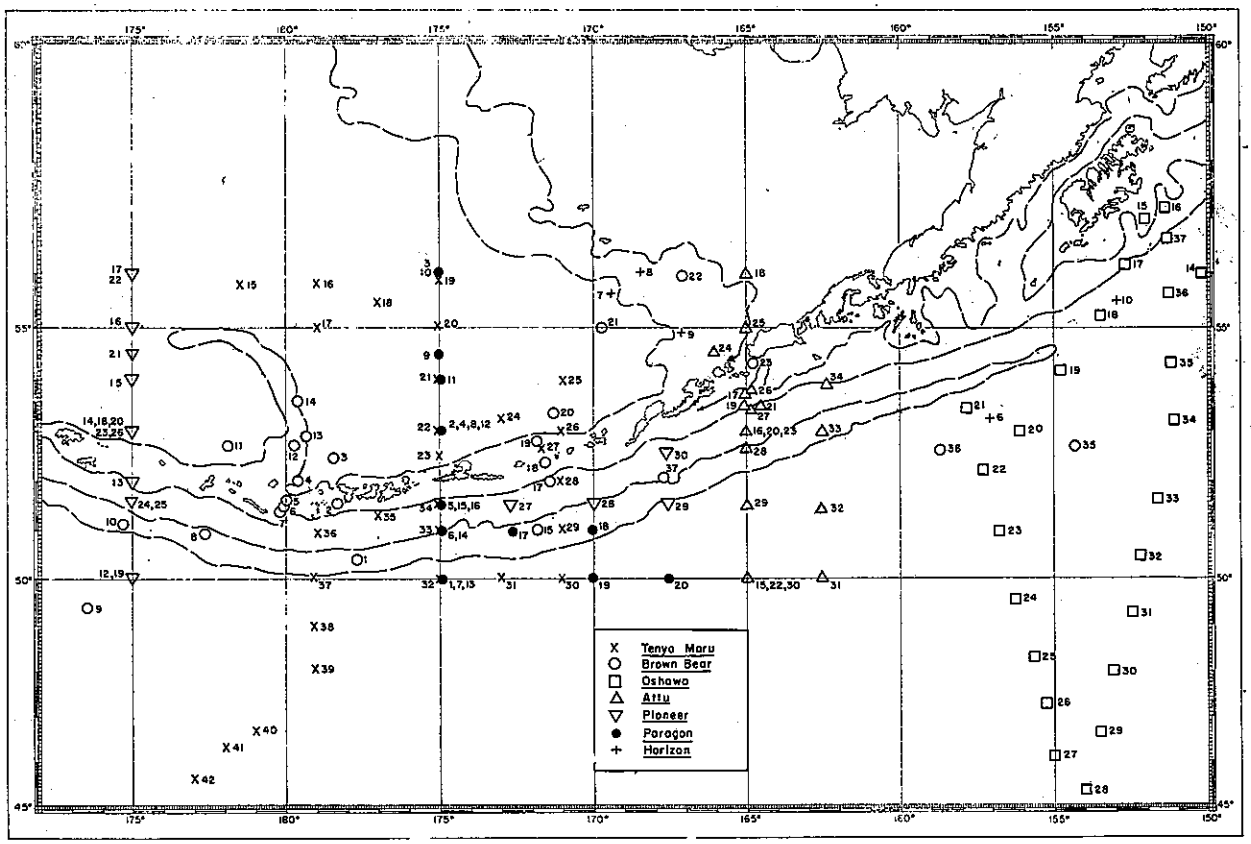

Figure 2.--Station positions, July 19 - August 31, 1957.

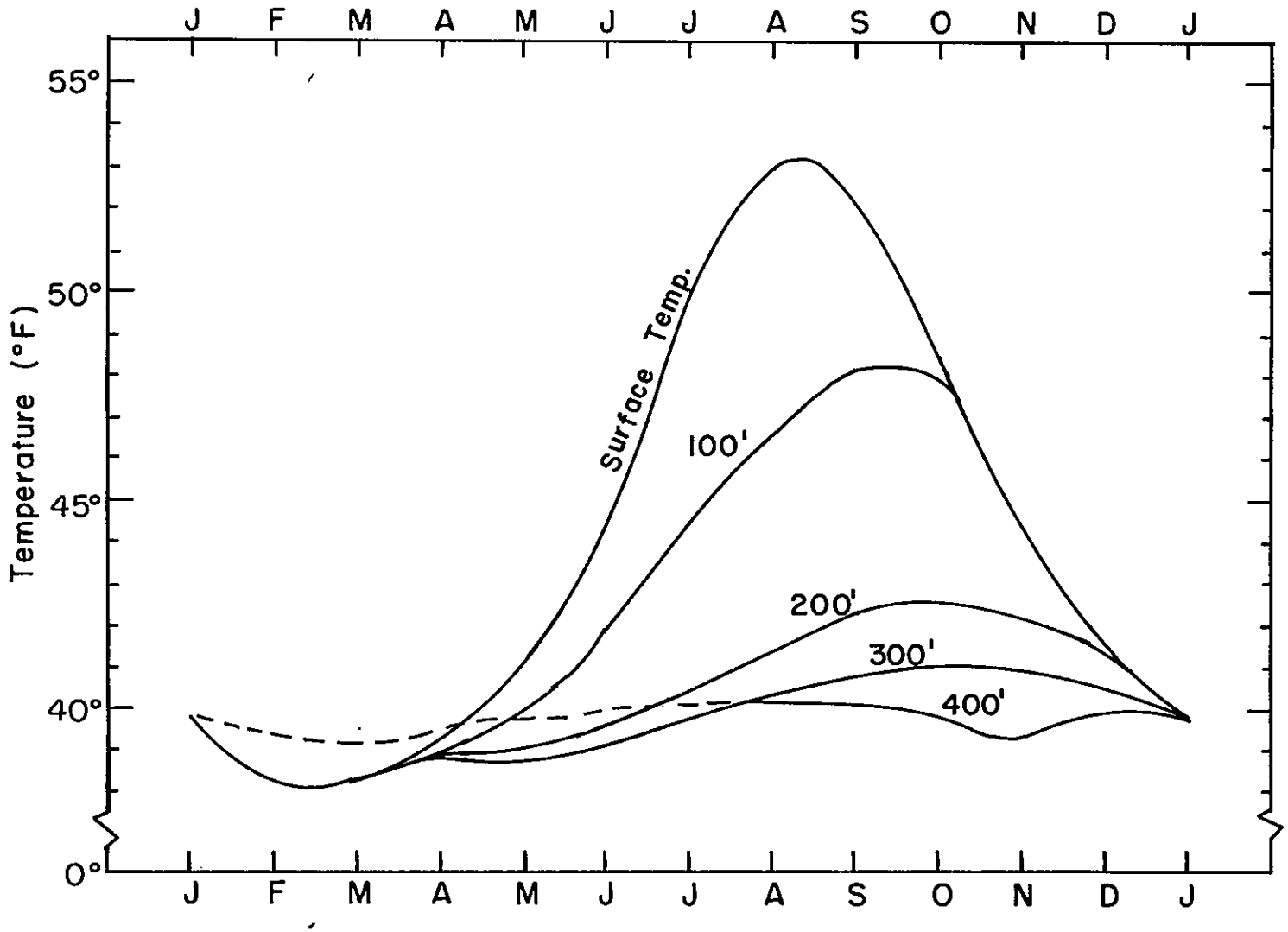

Figure 3.--Time series of mean temperature (°F.) for the area 50° - 55°N.; 160° - 165°W.; from Robinson (1957).

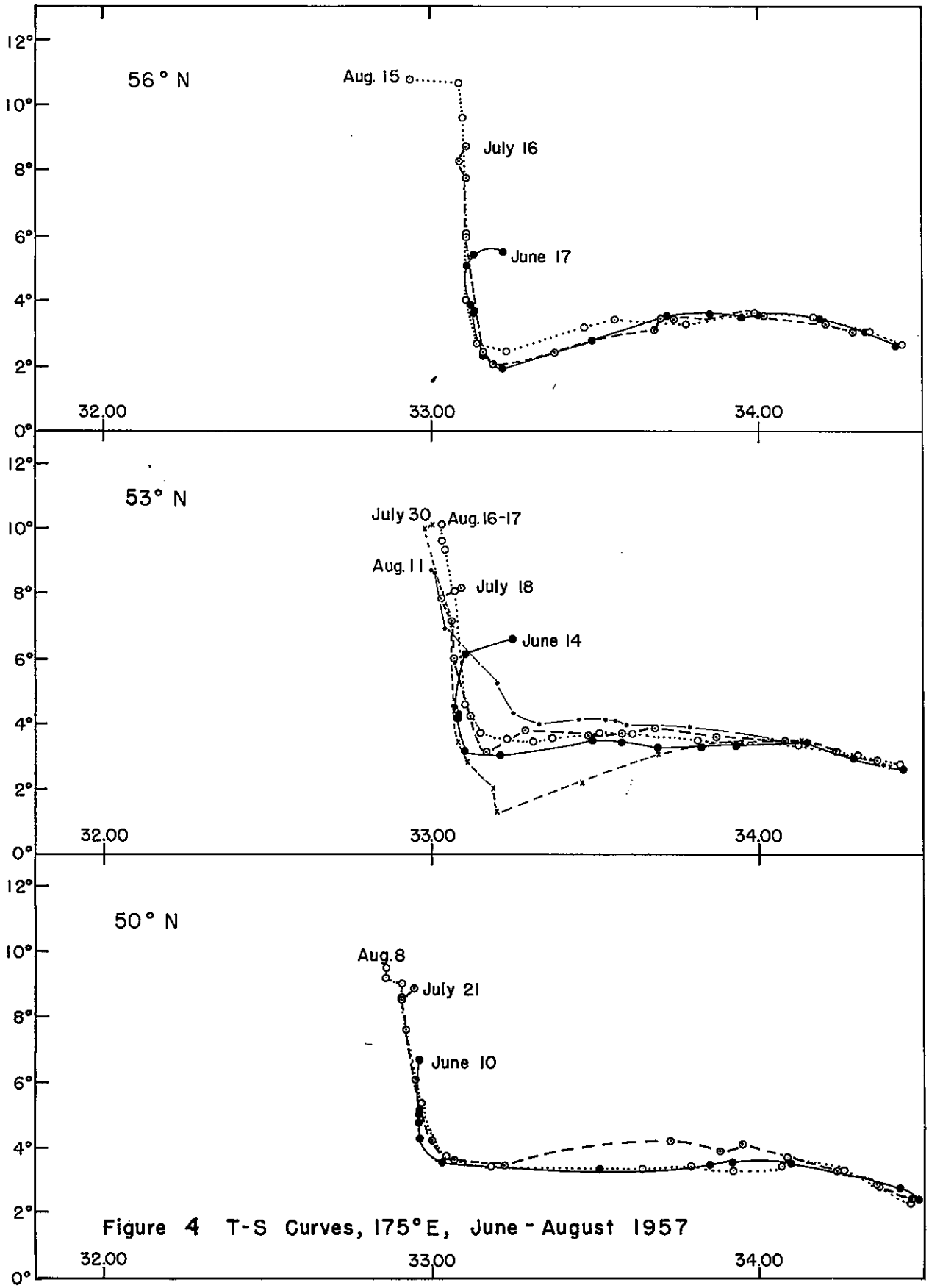

Figure 4 T-S Curves, 175°E, June - August 1957

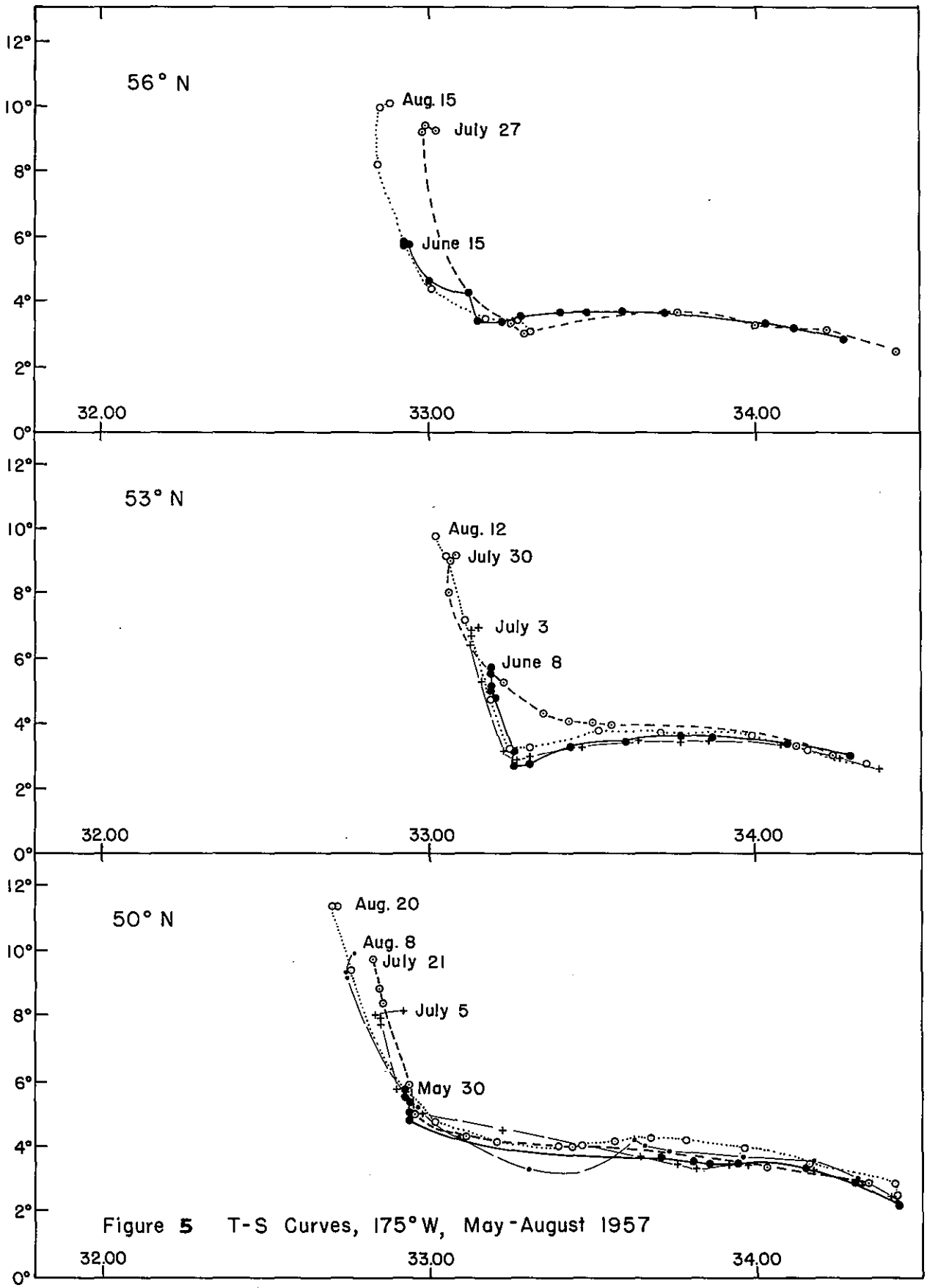

Figure 5 T-S Curves, 175° W, May - August 1957

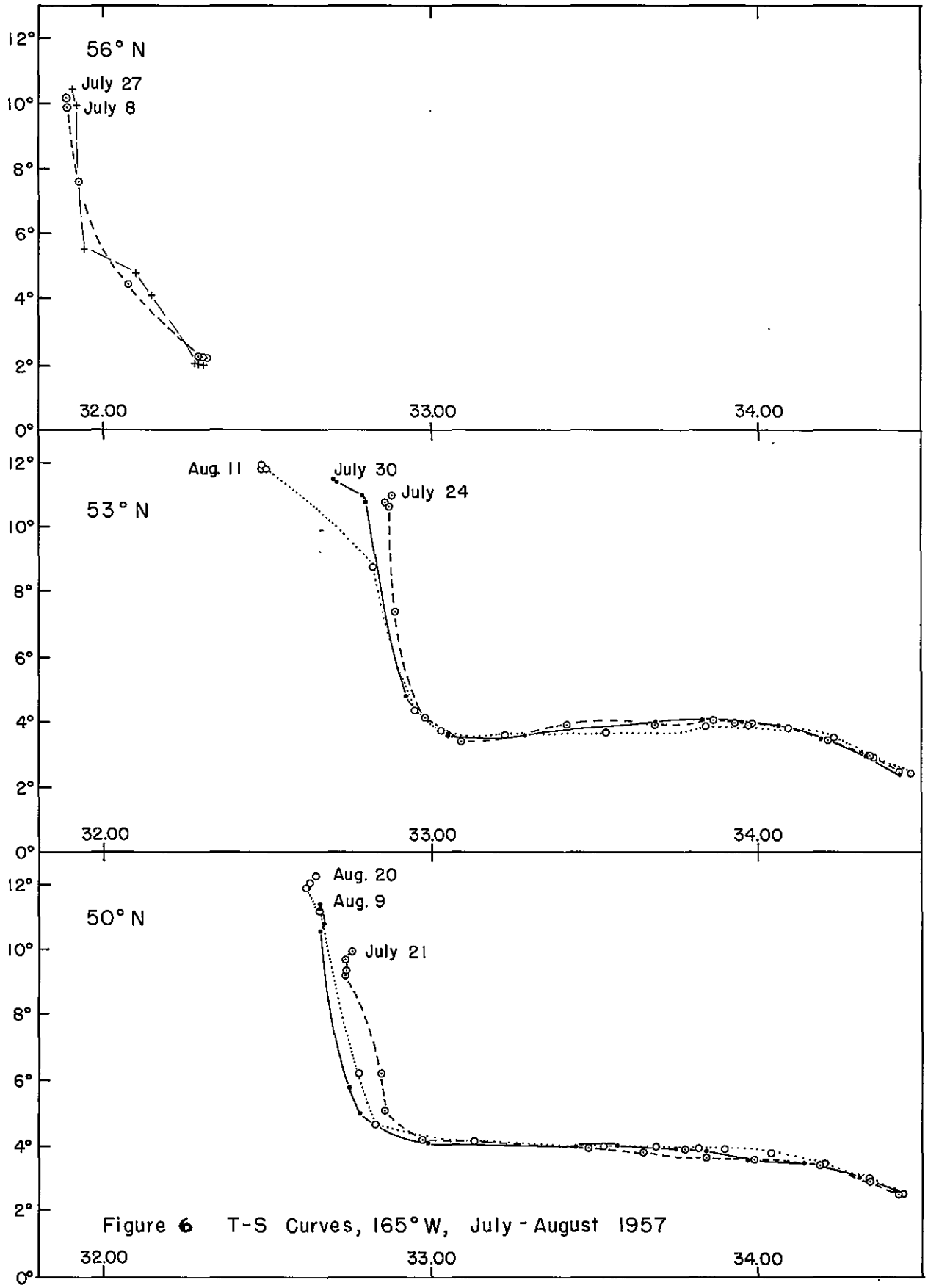

Figure 6 T-S Curves, 165° W, July - August 1957

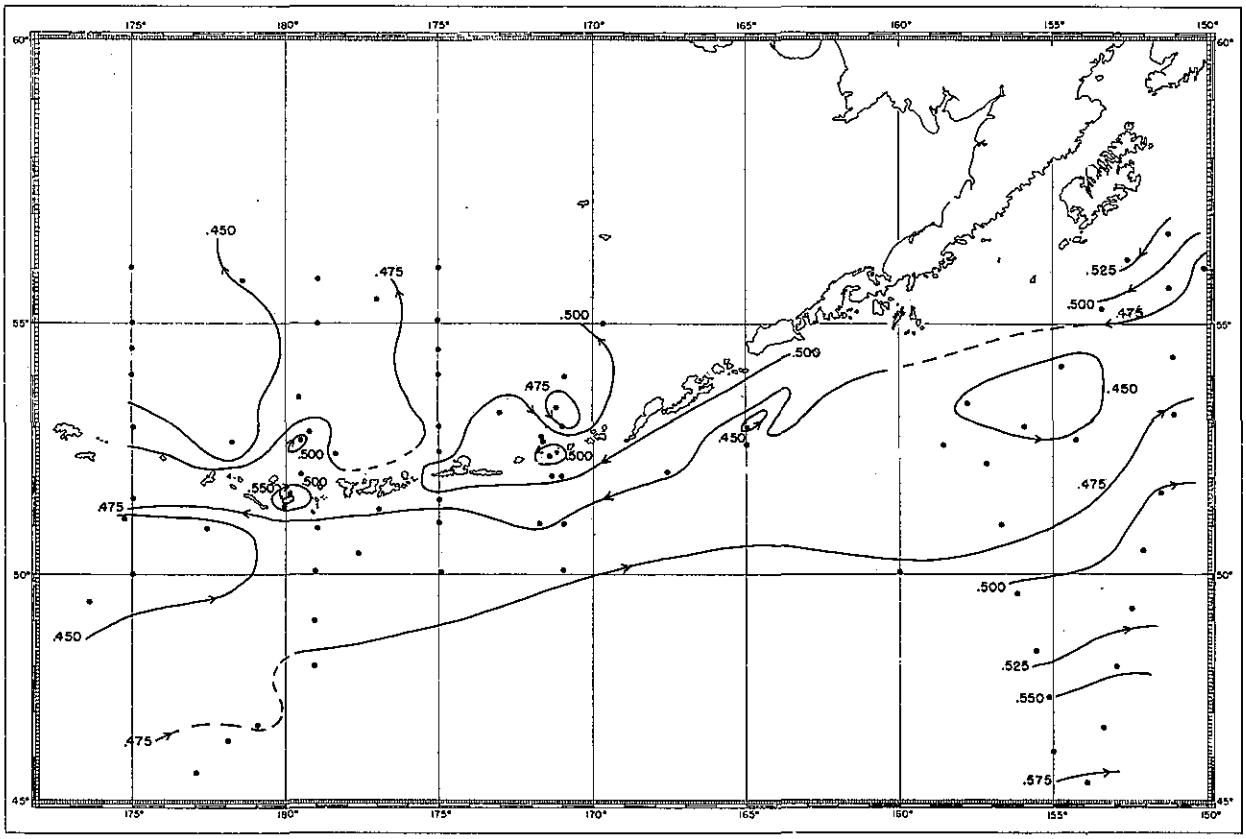

Figure 7.--Anomaly of geopotential topography, 0/300 db. Points indicate station positions.

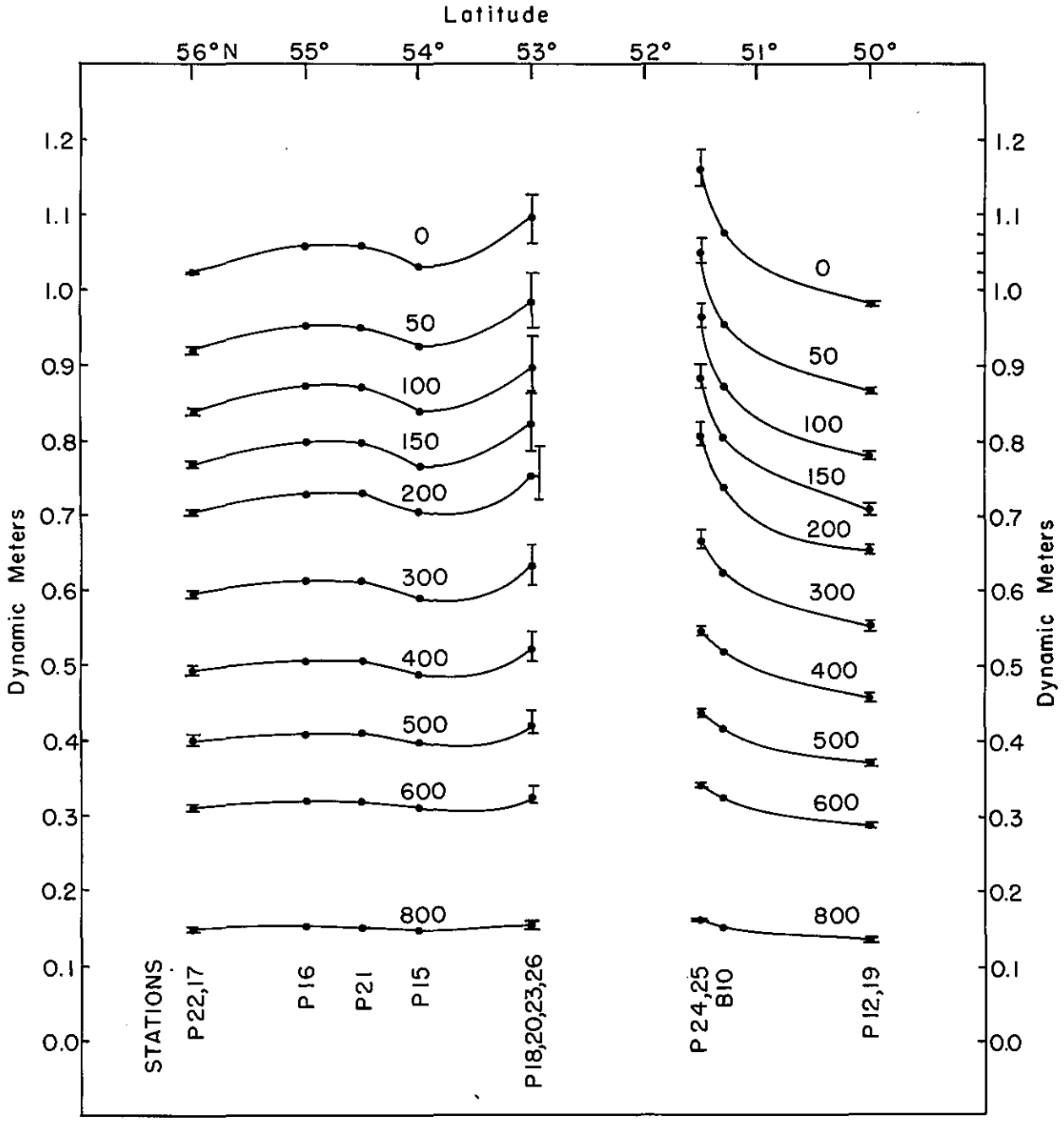

Figure 8.--Geopotential anomaly of the isobaric surfaces in dynamic meters relative to the 1000 db surface along 175°E. longitude, August 1957. Points indicate computed values. Range of dynamic heights shown by vertical bars.

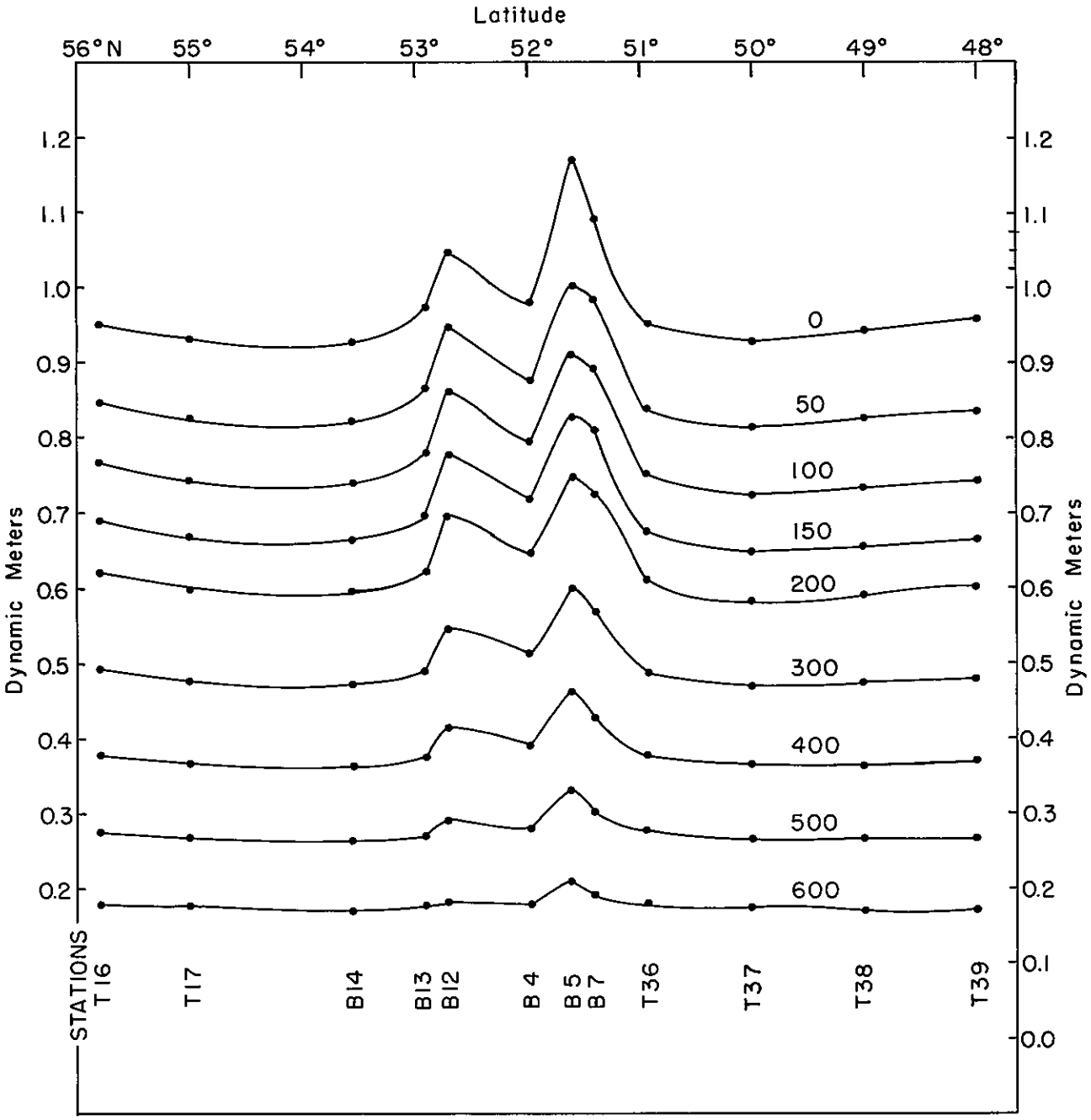

Figure 9.--Smoothed geopotential anomaly of the isobaric surfaces in dynamic meters relative to the 800 db. surface along 179°W. longitude, July-August, 1957. Points represent computed values.

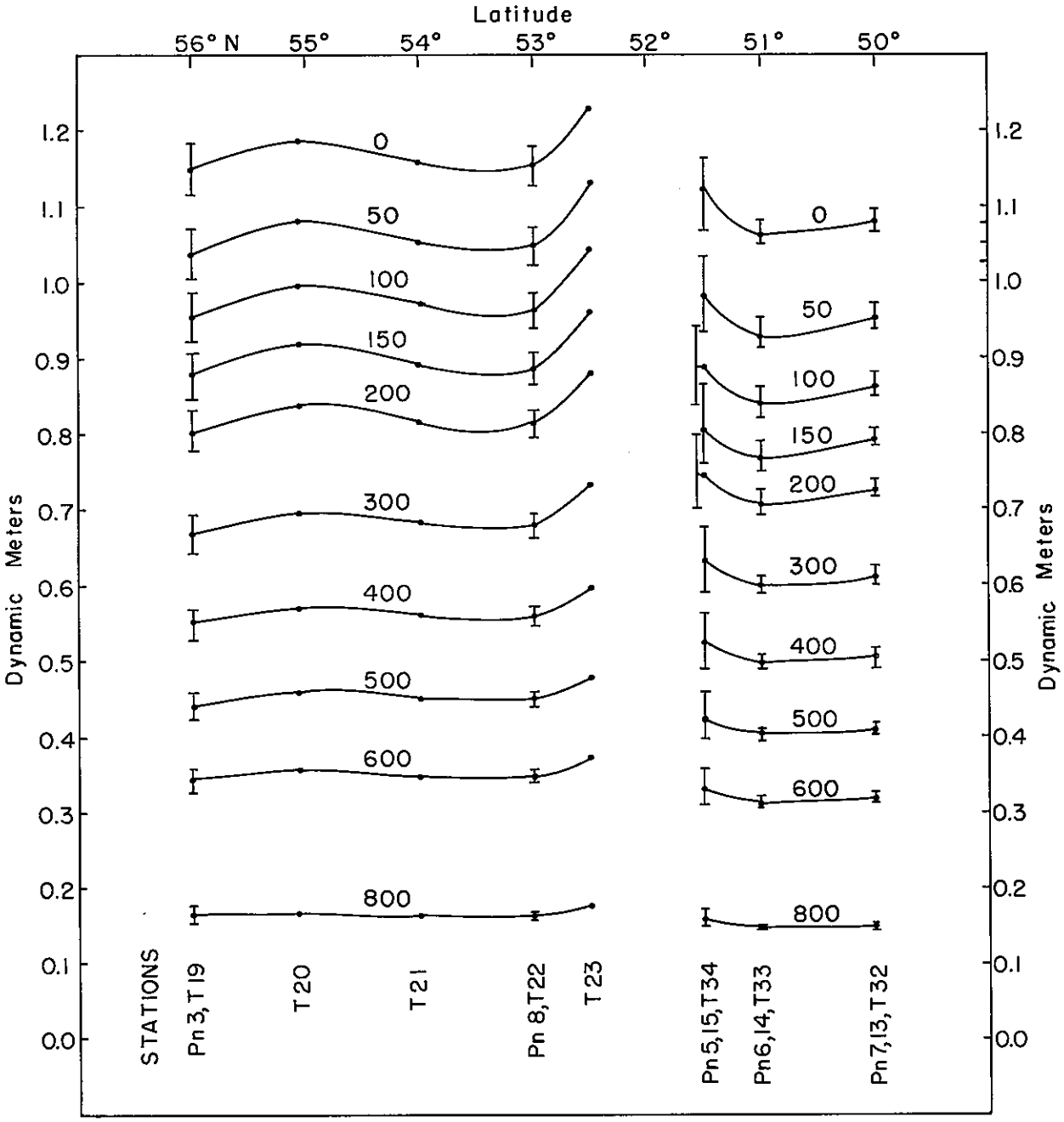

Figure 10.--Geopotential anomaly of the isobaric surfaces in dynamic meters relative to the 1000 db surface along 175 W. longitude, July-August, 1957. Points indicate computed values. Range of dynamic heights shown by vertical bars.

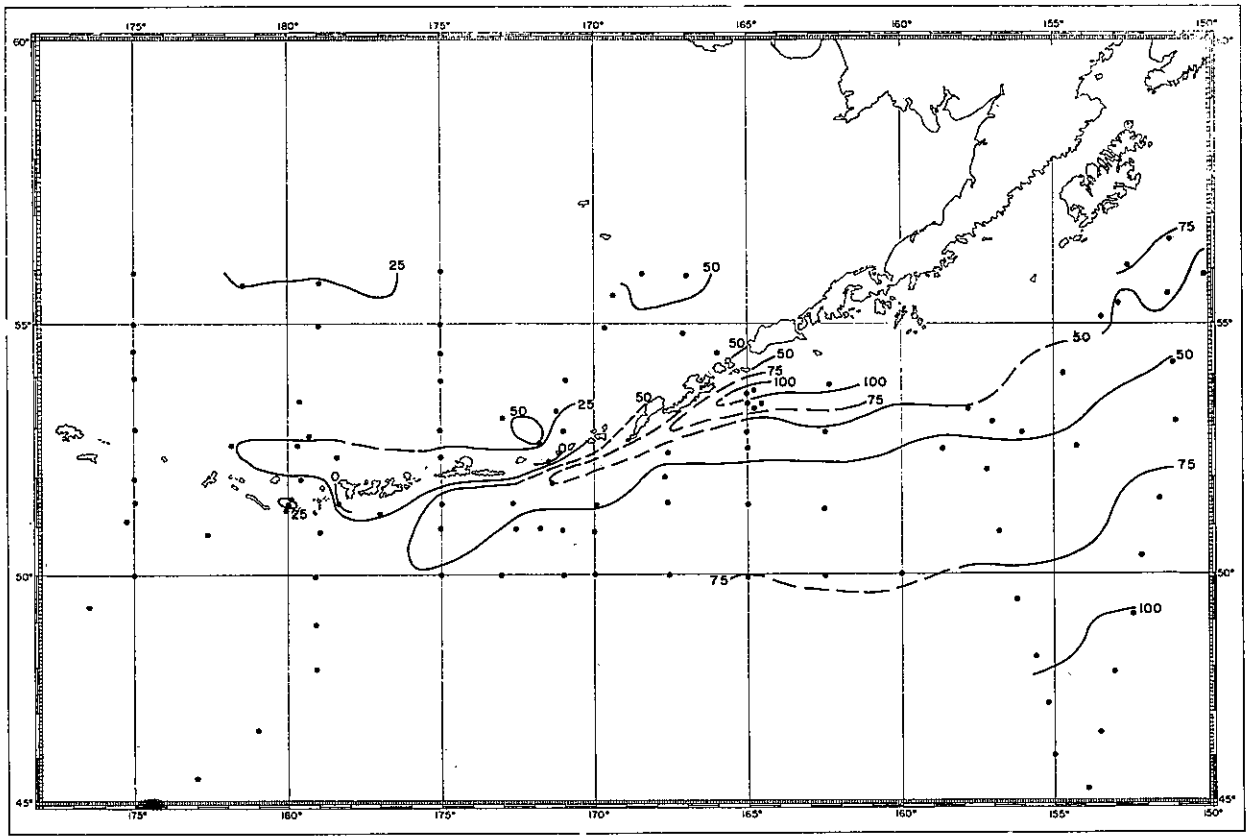

Figure 11.--Depth (meters) of the 26.0 sigma-t surface. Dots indicate station positions.

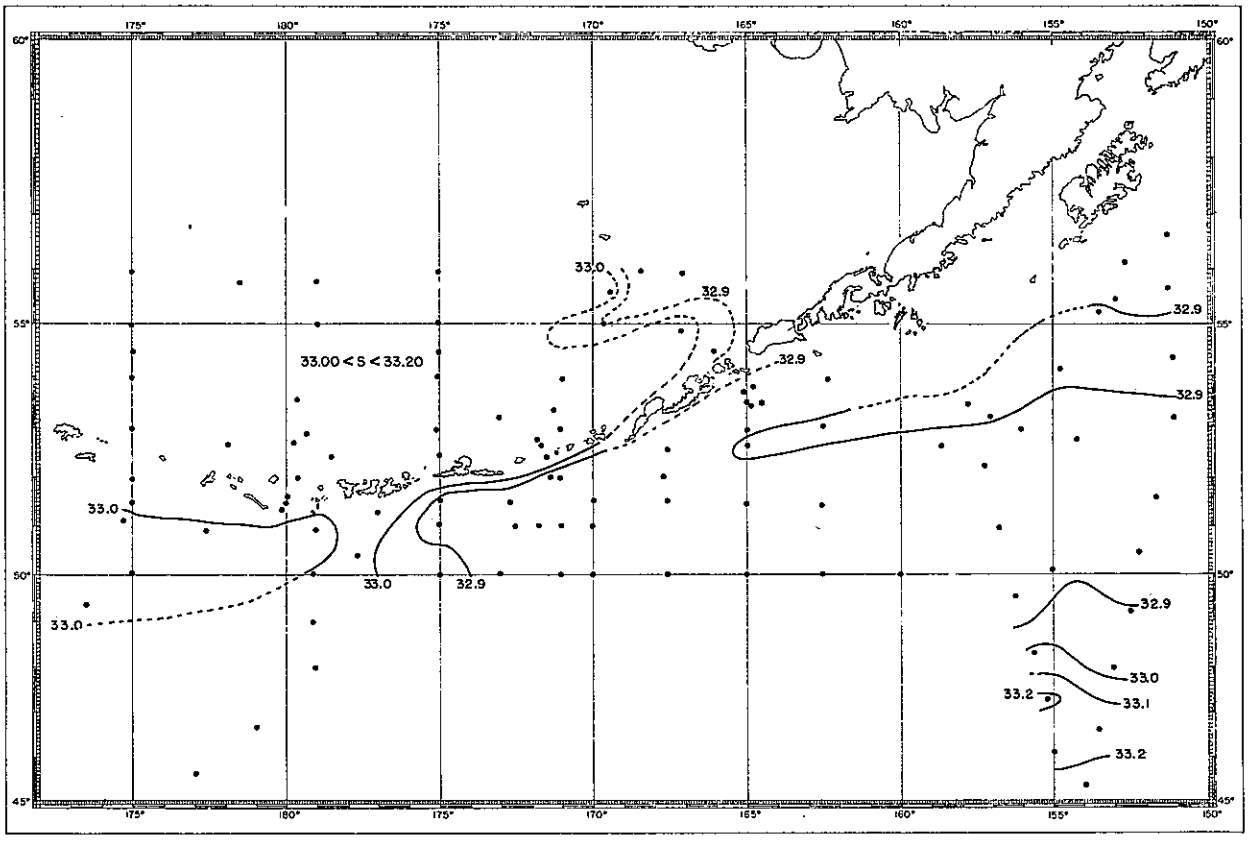

Figure 12.--Salinity (°/oo) on the 26.0 sigma-t surface. Dots indicate station positions.

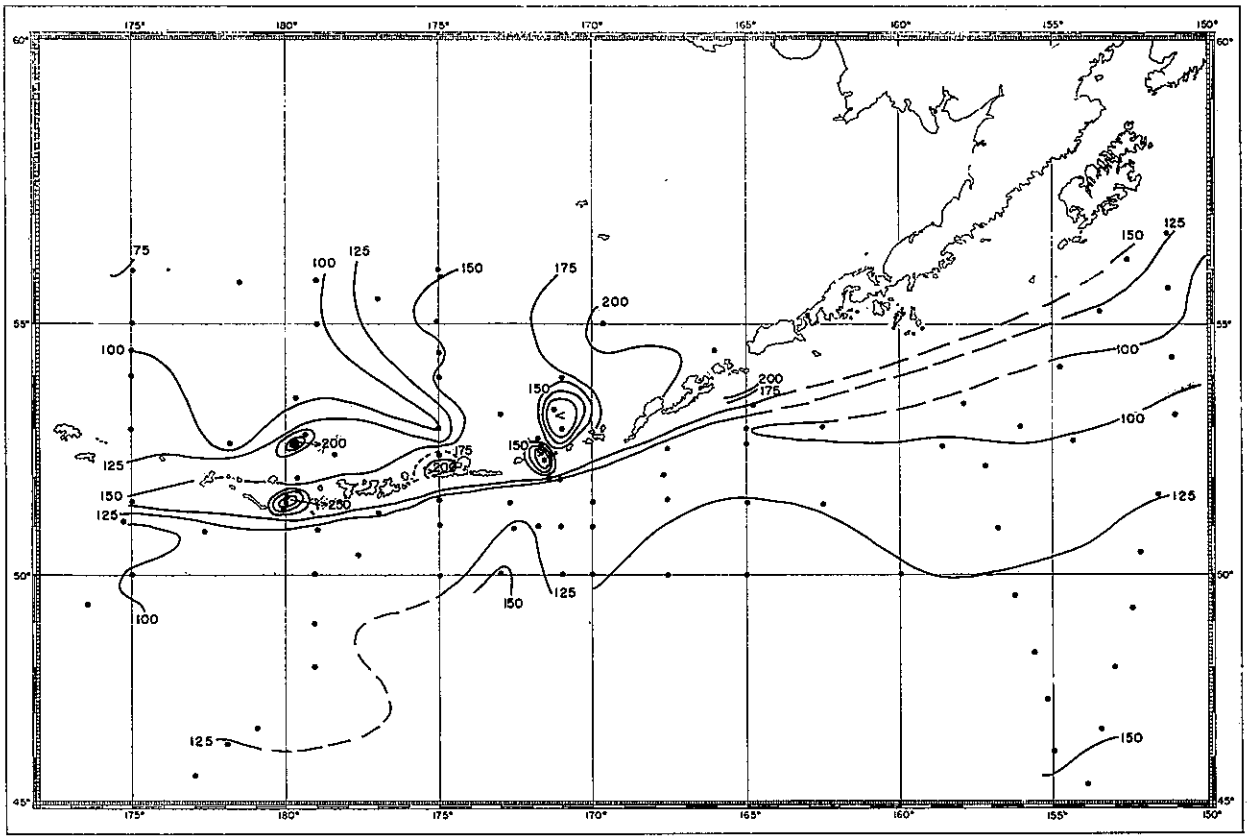

Figure 13.--Depth (meters) of the 26.5 sigma-t surface. Dots indicate station positions.

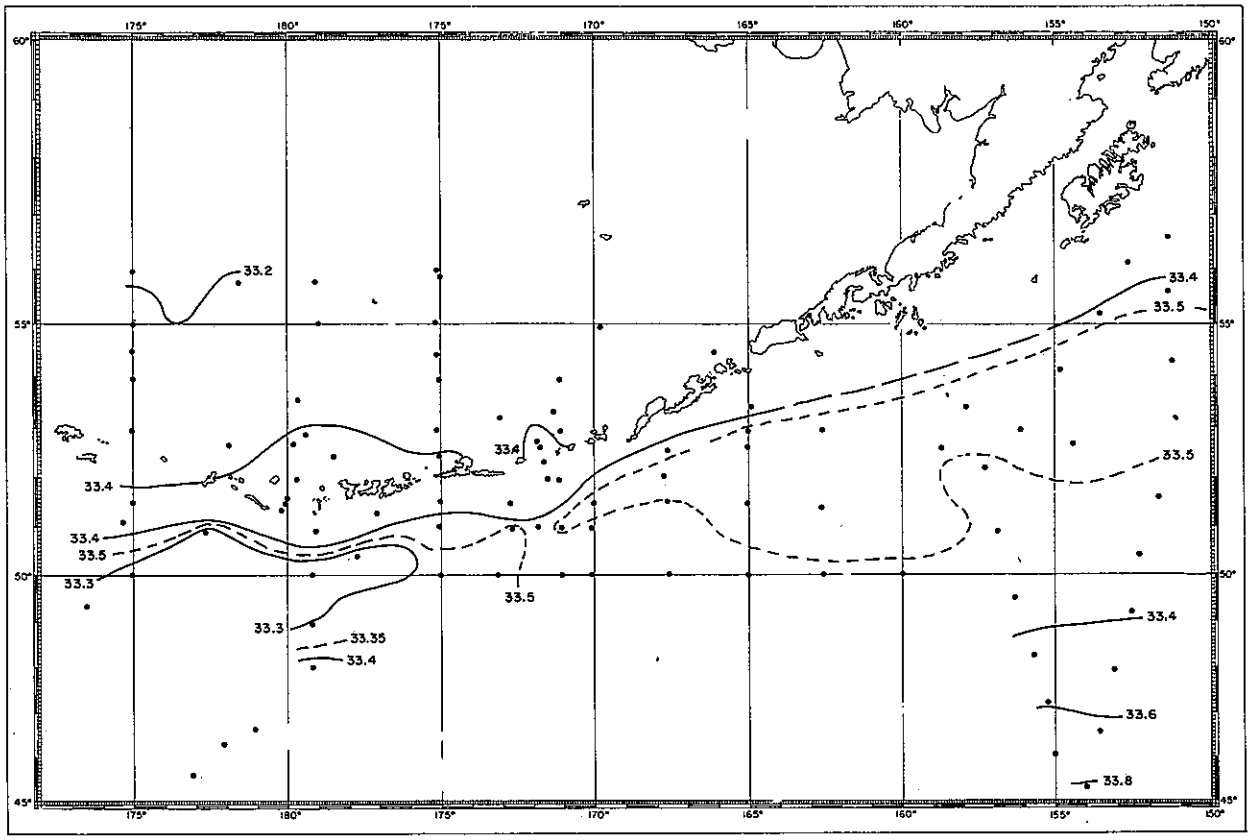

Figure 14.--Salinity (°/oo) on the 26.5 sigma-t surface. Dots indicate station positions.

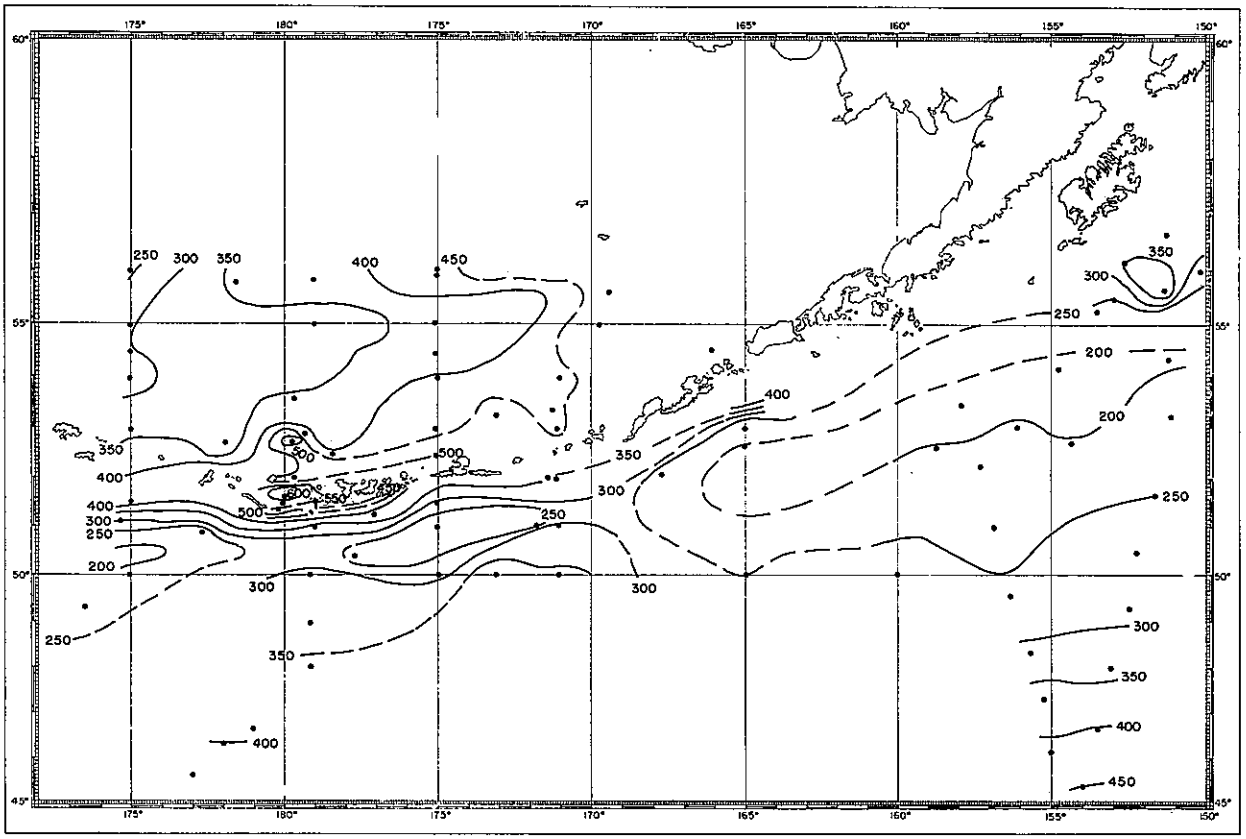

Figure 15.--Depth (meters) of 27.0 sigma-t surface. Dots indicate station positions.

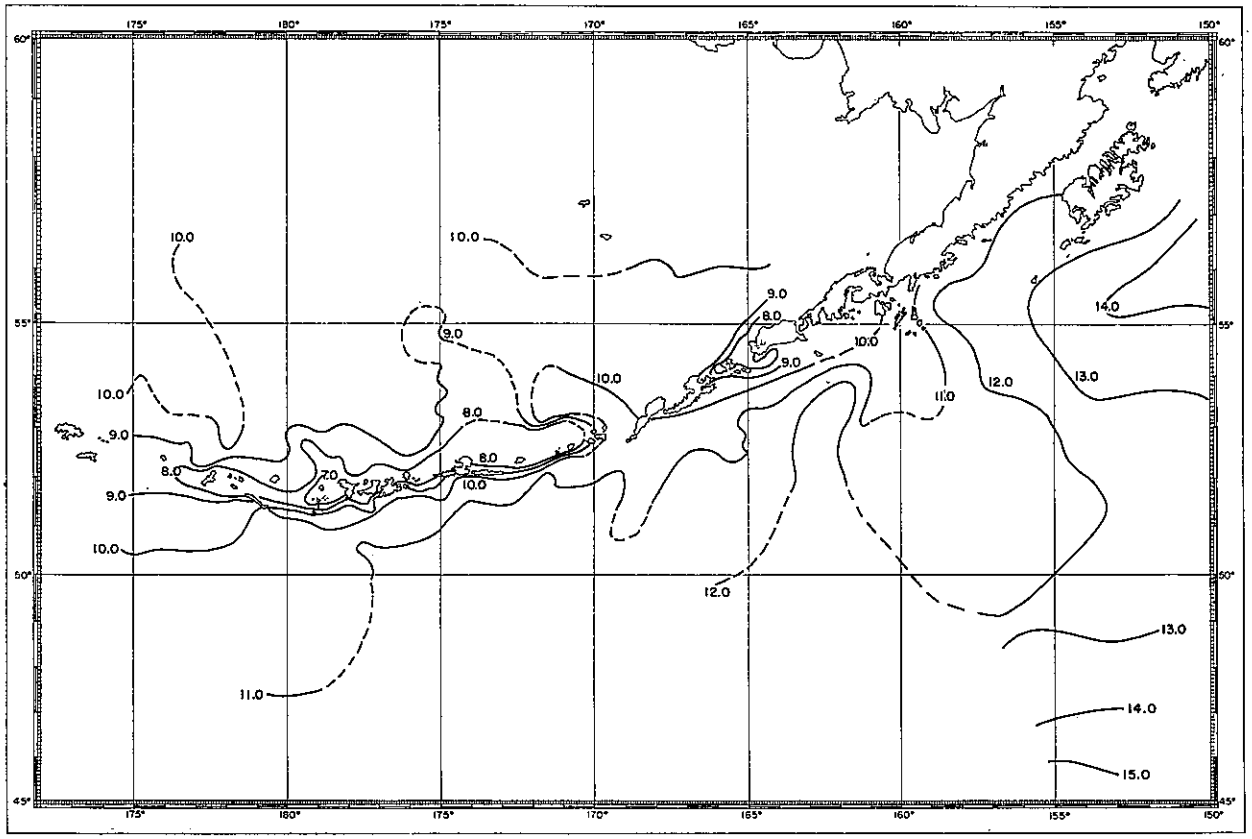

Figure 16.--Surface temperature (^{o}C.) July-August, 1957.

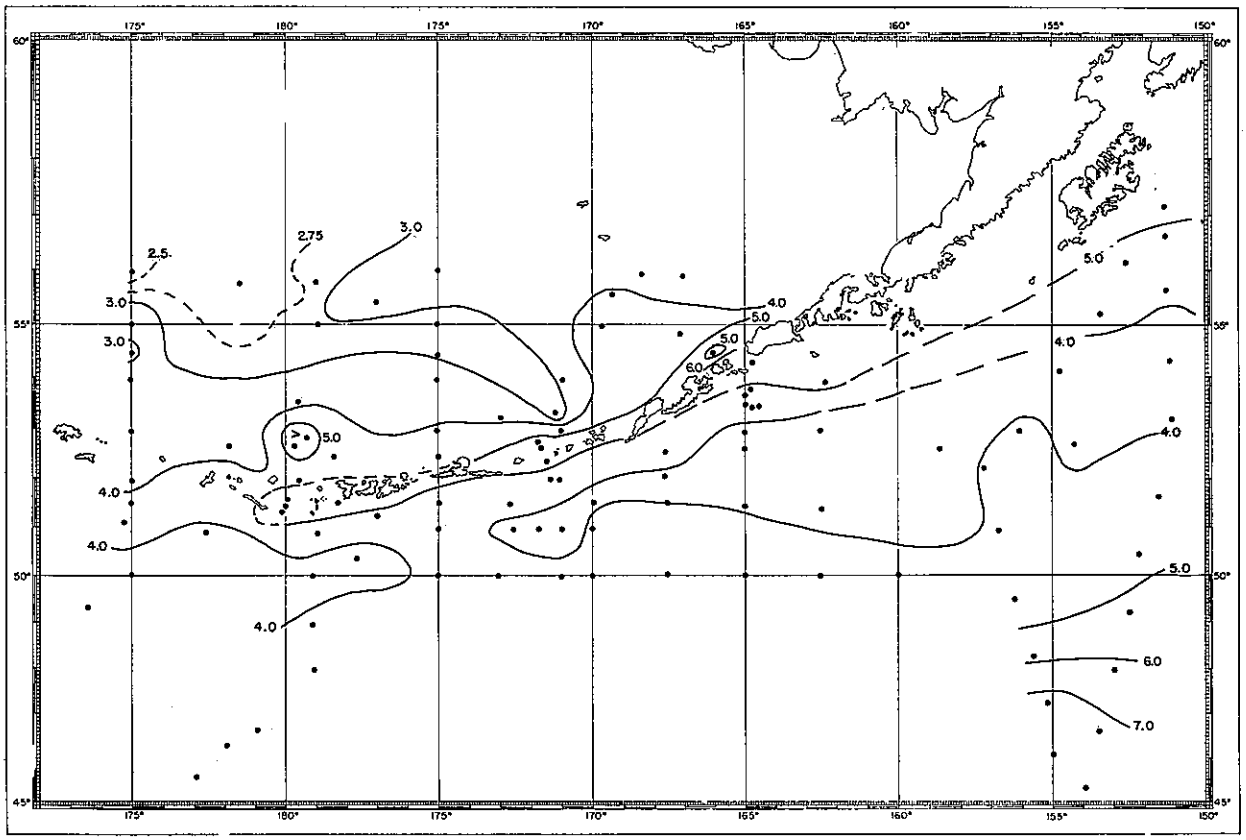

Figure 17.--Temperature (°C.) at 100 meters, July-August, 1957. Dots indicate station positions.

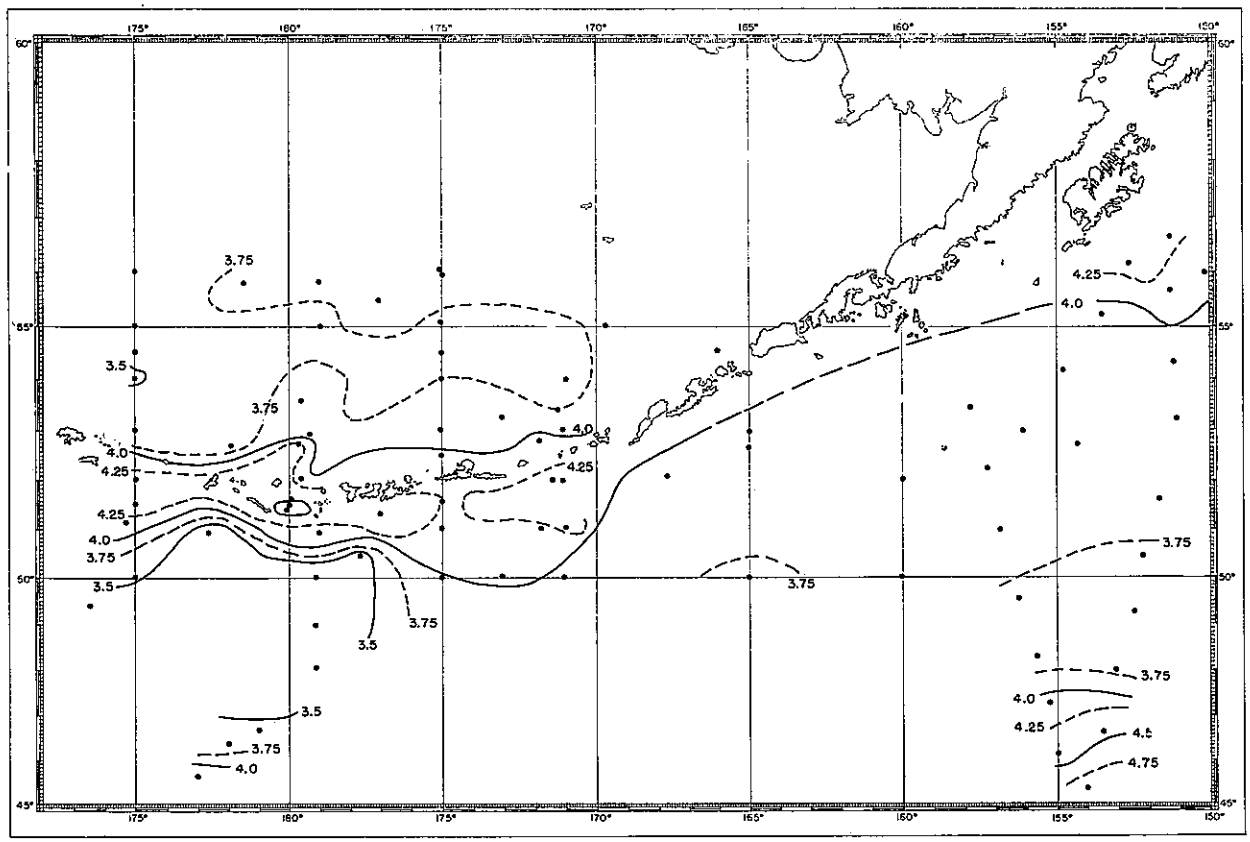

Figure 18.--Temperature (°C.) at 300 meters, July-August, 1957. Dots indicate station positions.

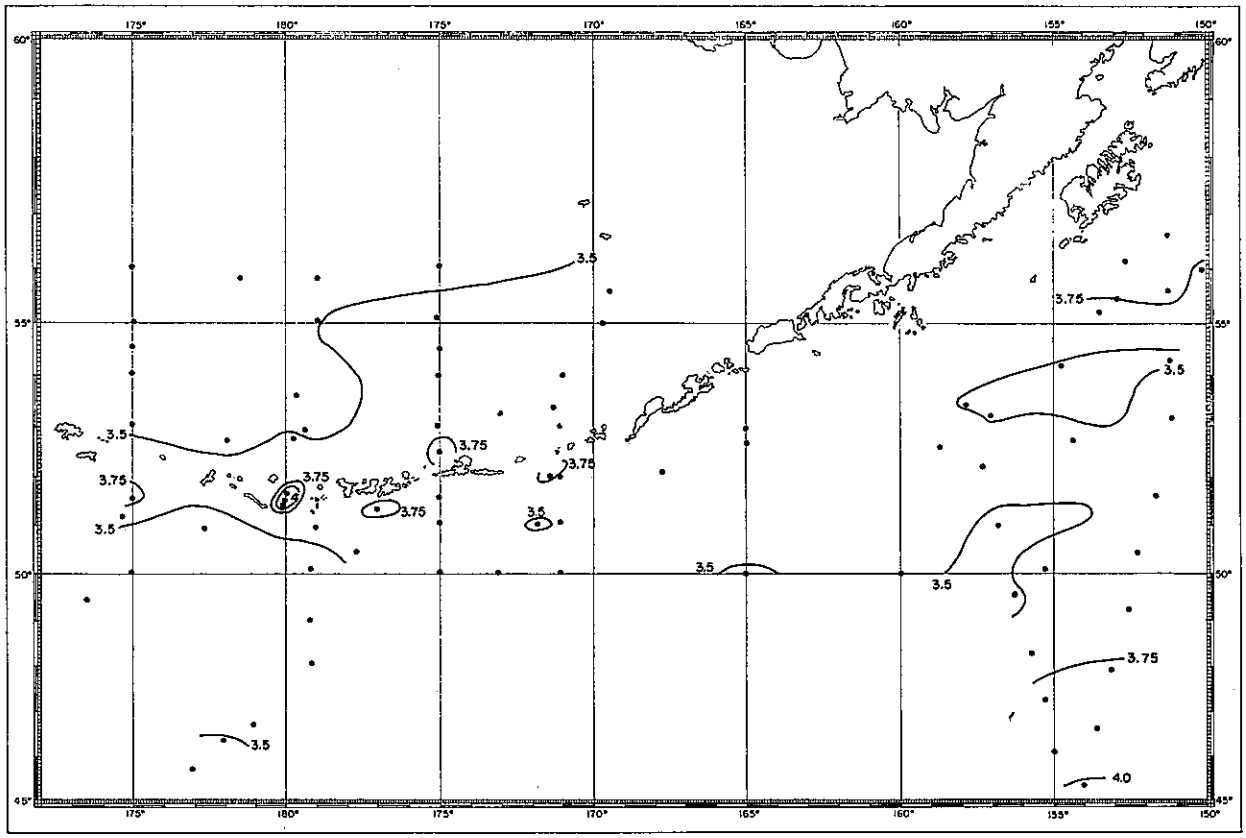

Figure 19.--Temperature (°C.) at 500 meters, July-August, 1957. Dots indicate station positions.

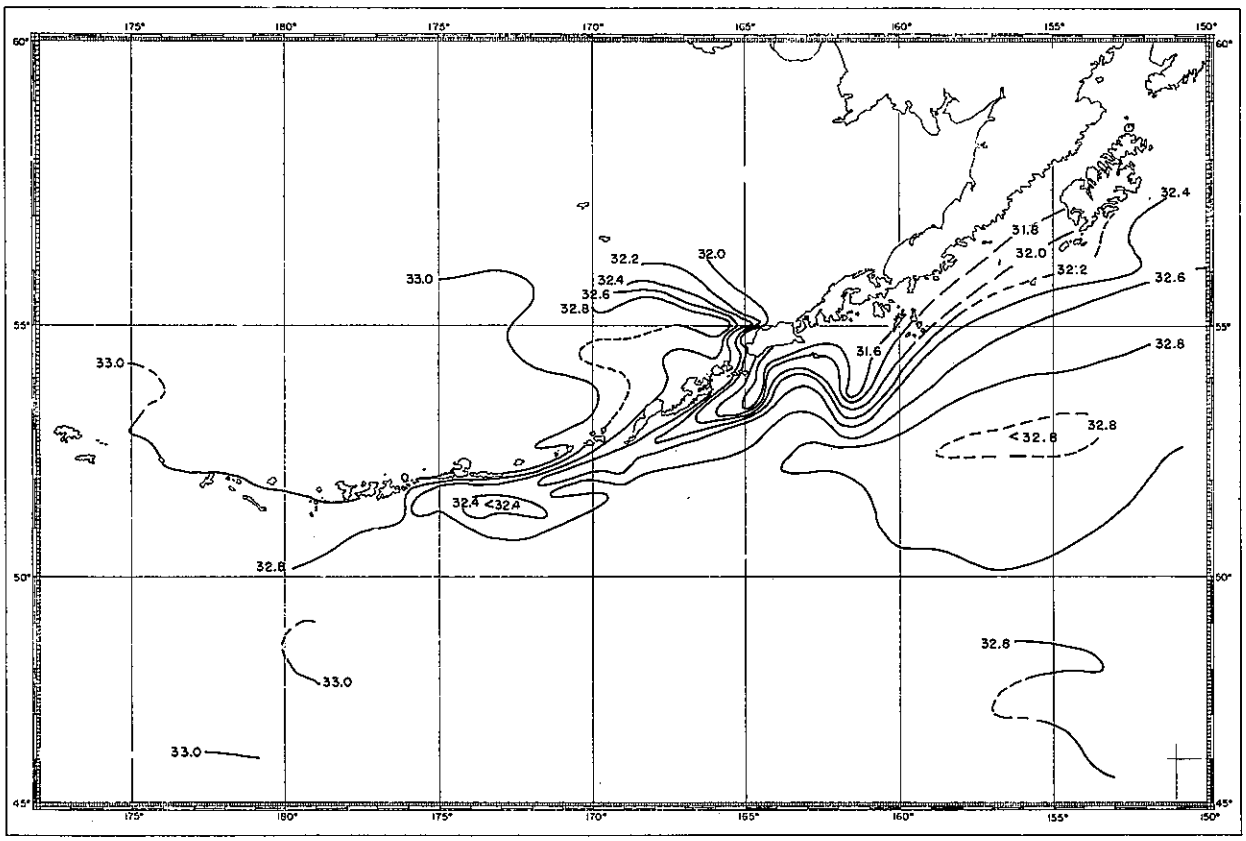

Figure 20.--Surface salinity (°/oo), July-August, 1957.

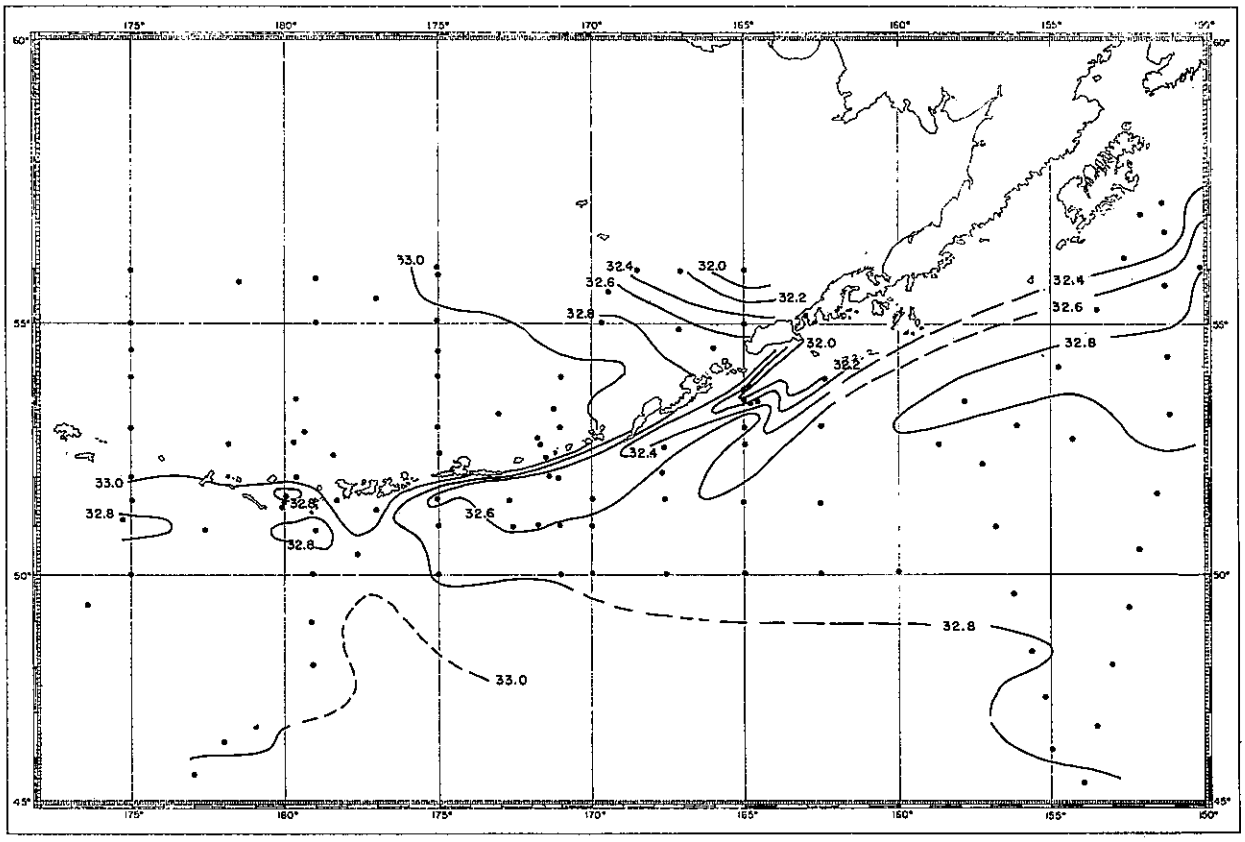

Figure 21.--Salinity (°/oo) at 10 meters, July-August, 1957. Dots indicate station positions.

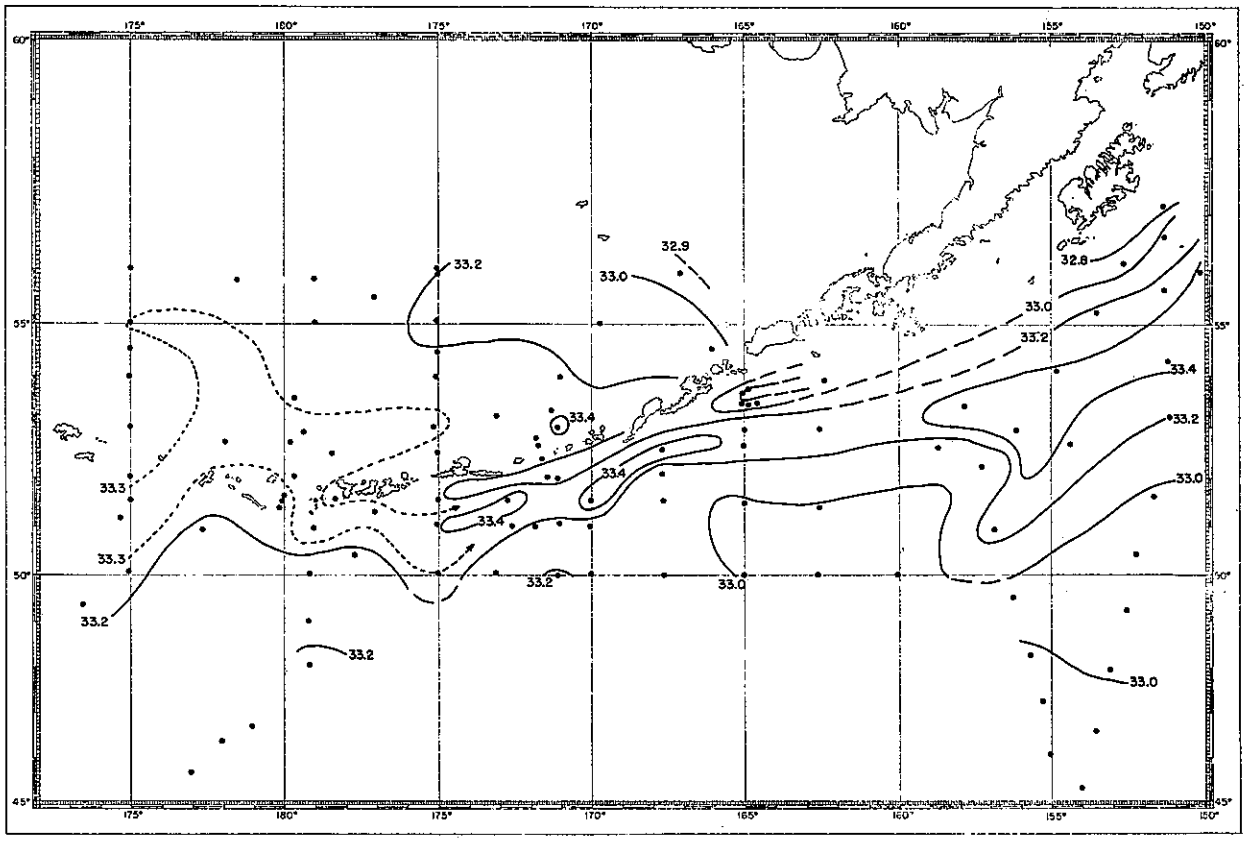

Figure 22.--Salinity (°/oo) at 100 meters, July-August, 1957. Dots indicate station positions.

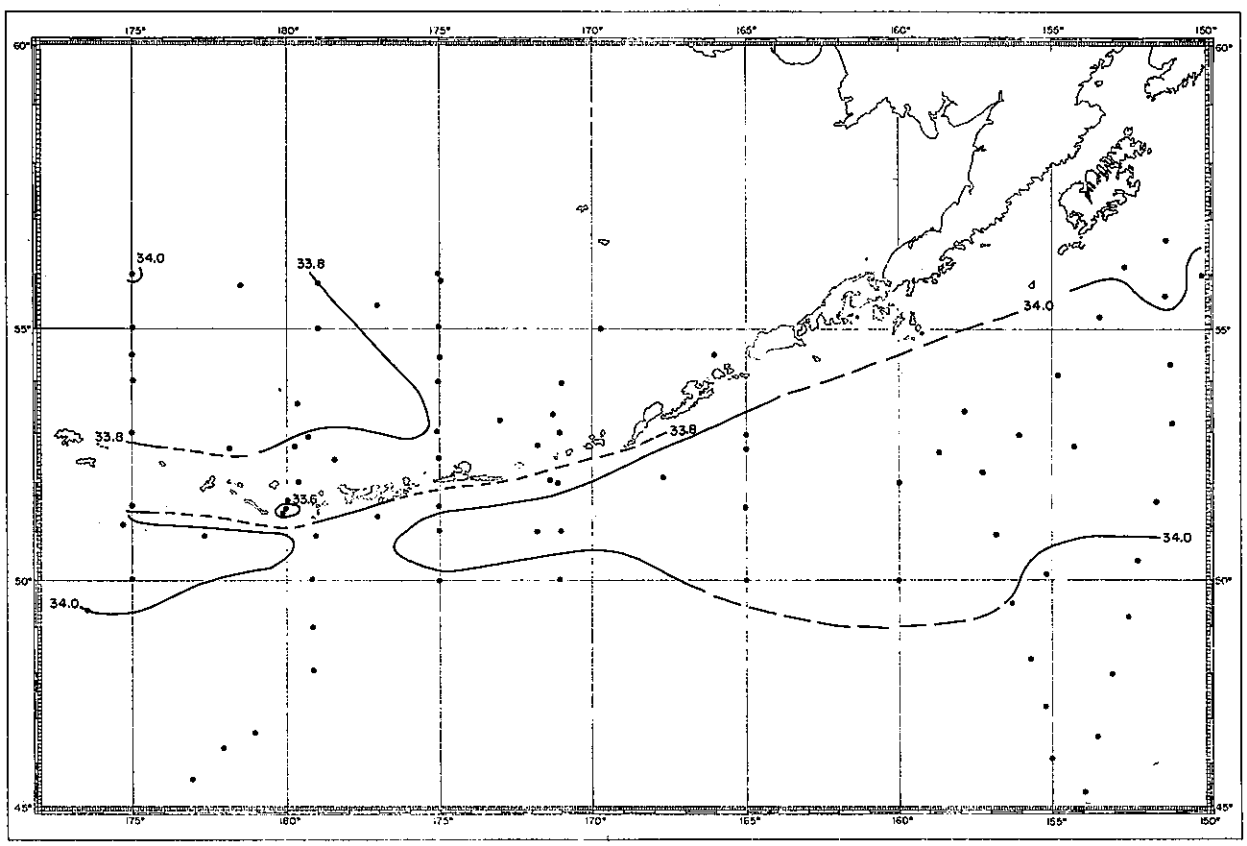

Figure 23.--Salinity (°/oo) at 300 meters, July-August, 1957. Dots indicate station positions.

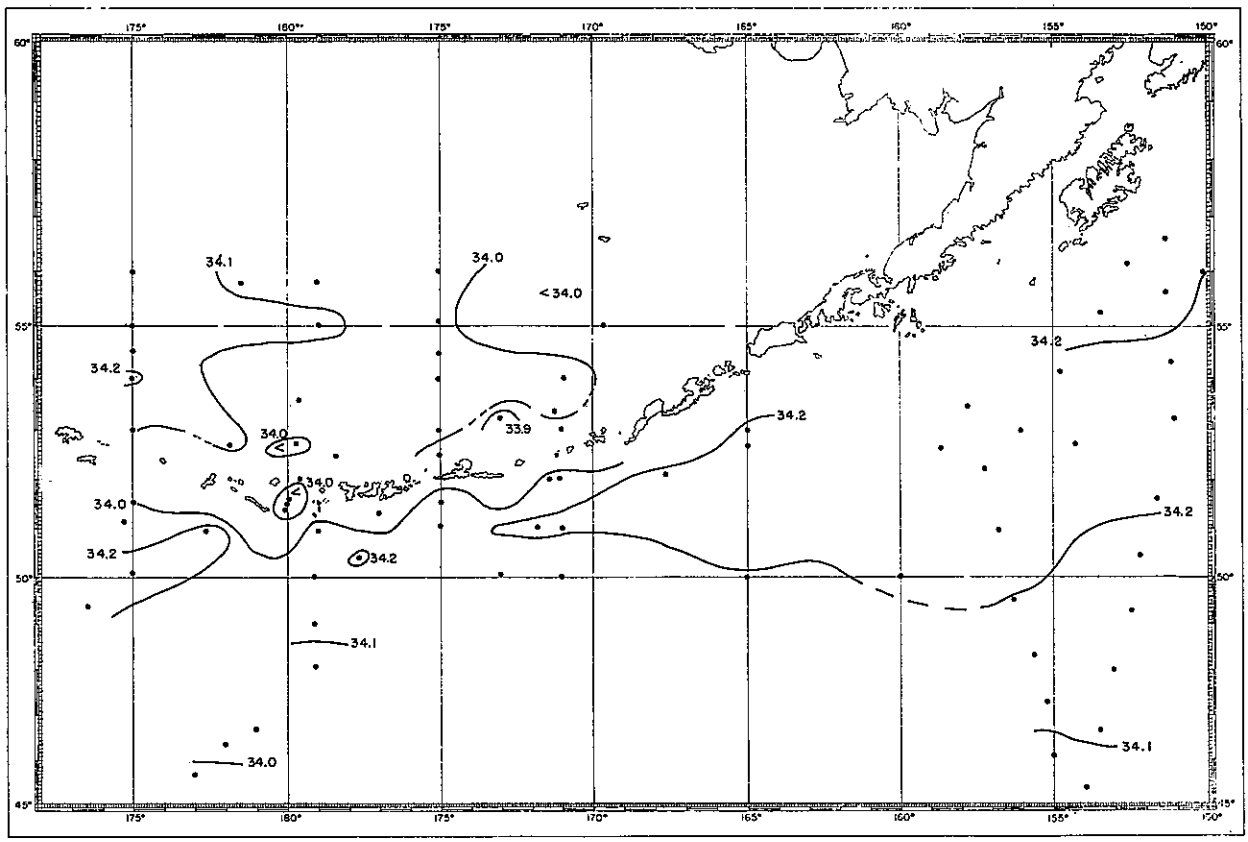

Figure 24.--Salinity (°/oo) at 500 meters, July-August, 1957. Dots indicate station positions.

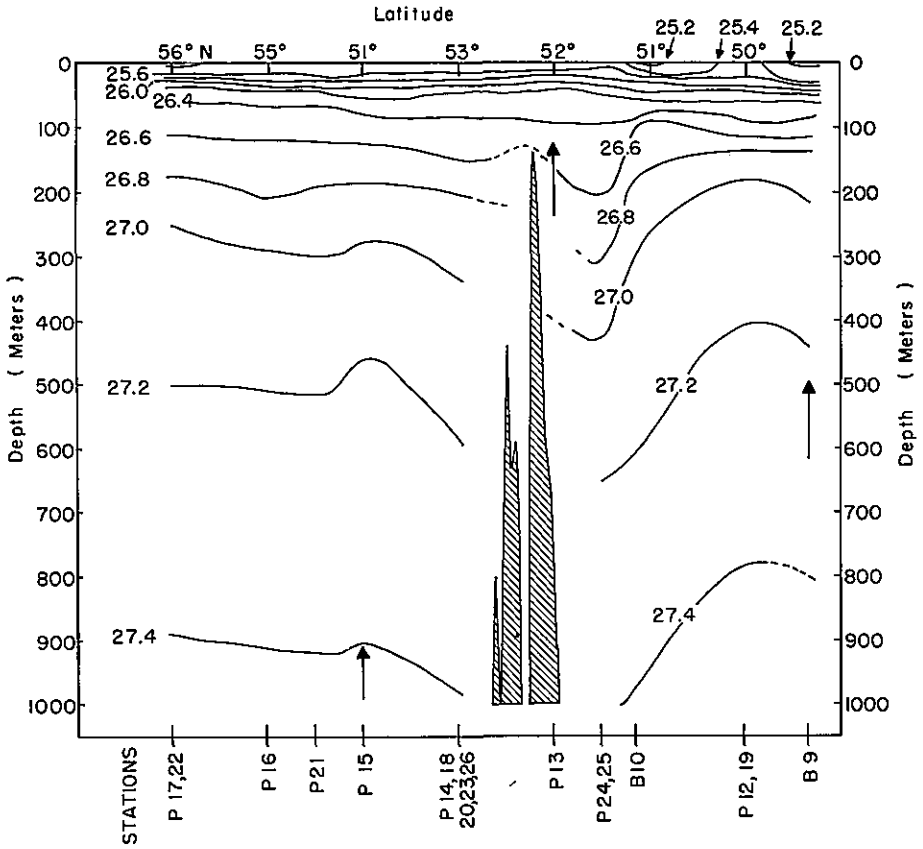

Figure 25.--Vertical distribution of sigma-t along 175°E. longitude, July-August, 1957. Large arrows indicate depths of Nansen bottle cast not reading 1000 meters.

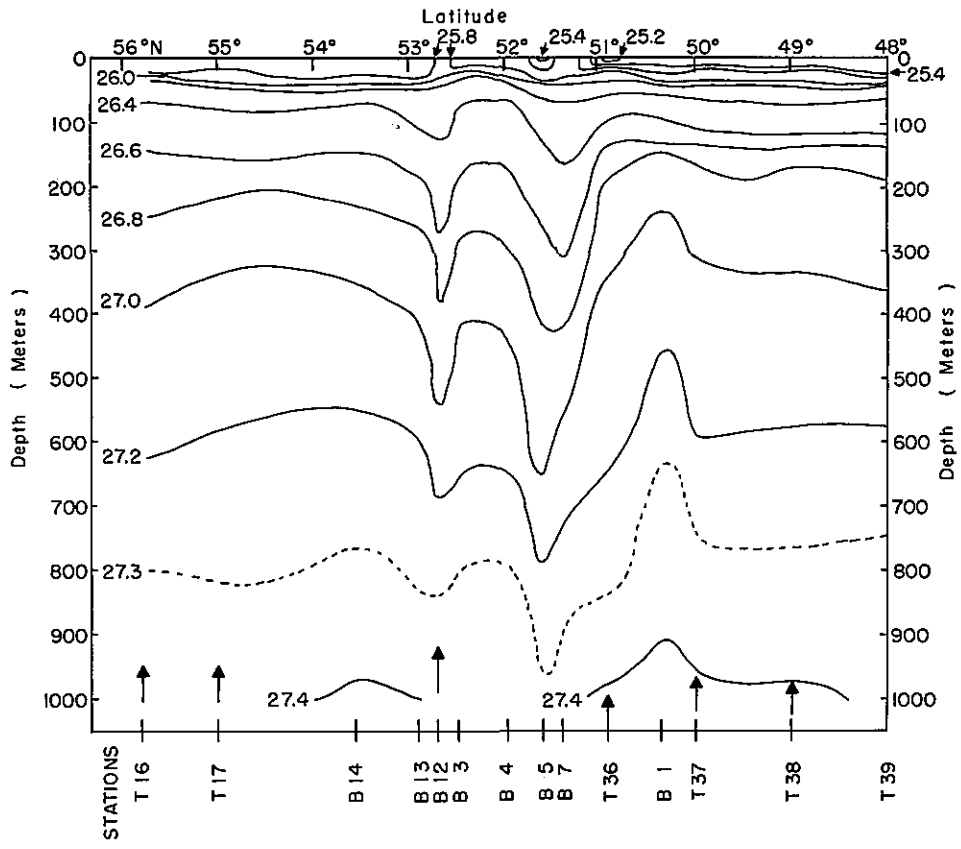

Figure 26.--Vertical distribution of sigma-t along 179°W. longitude, July-August, 1957. Large arrows indicate depths of Nansen bottle cast not reaching 1000 meters.

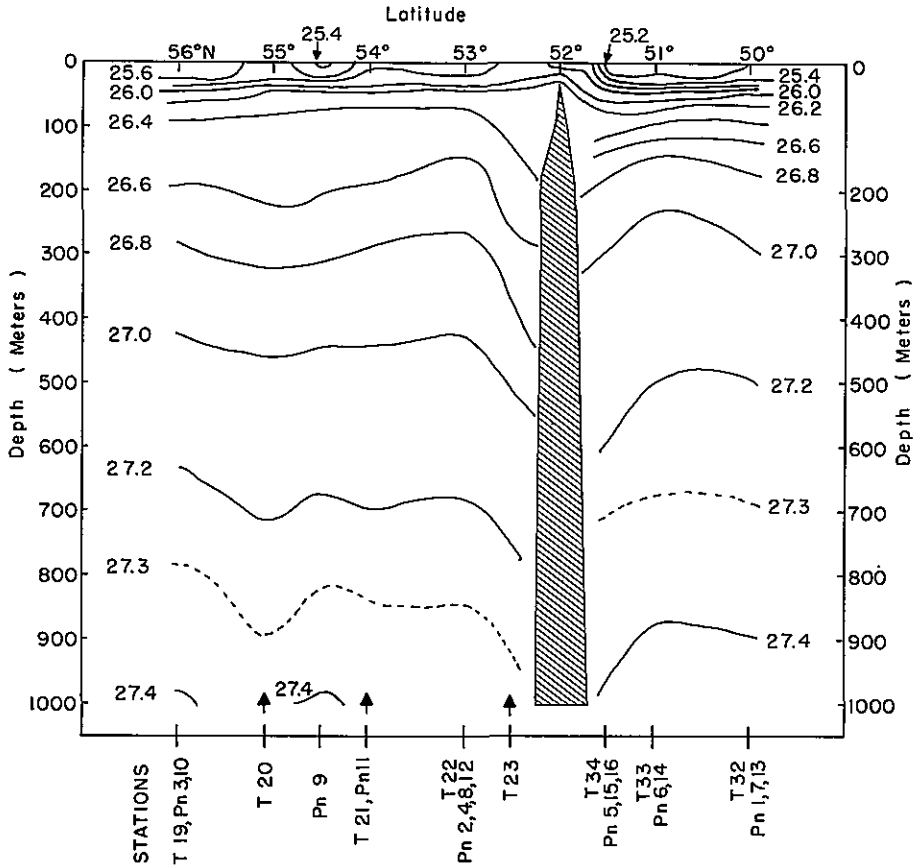

Figure 27.--Vertical distribution of sigma-t along 175°W. longitude, July-August, 1957. Large arrows indicate depths of Nansen bottle cast not reaching 1000 meters.

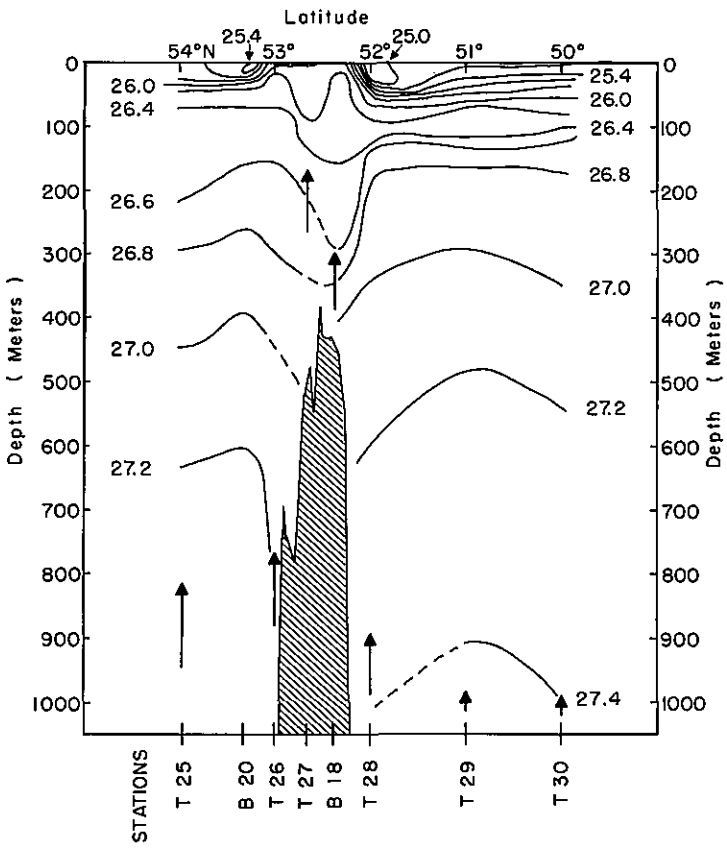

Figure 28.--Vertical distribution of sigma-t along 171°W. longitude, July-August, 1957. Large arrows indicate depths of Nansen bottle cast not reaching 1000 meters.

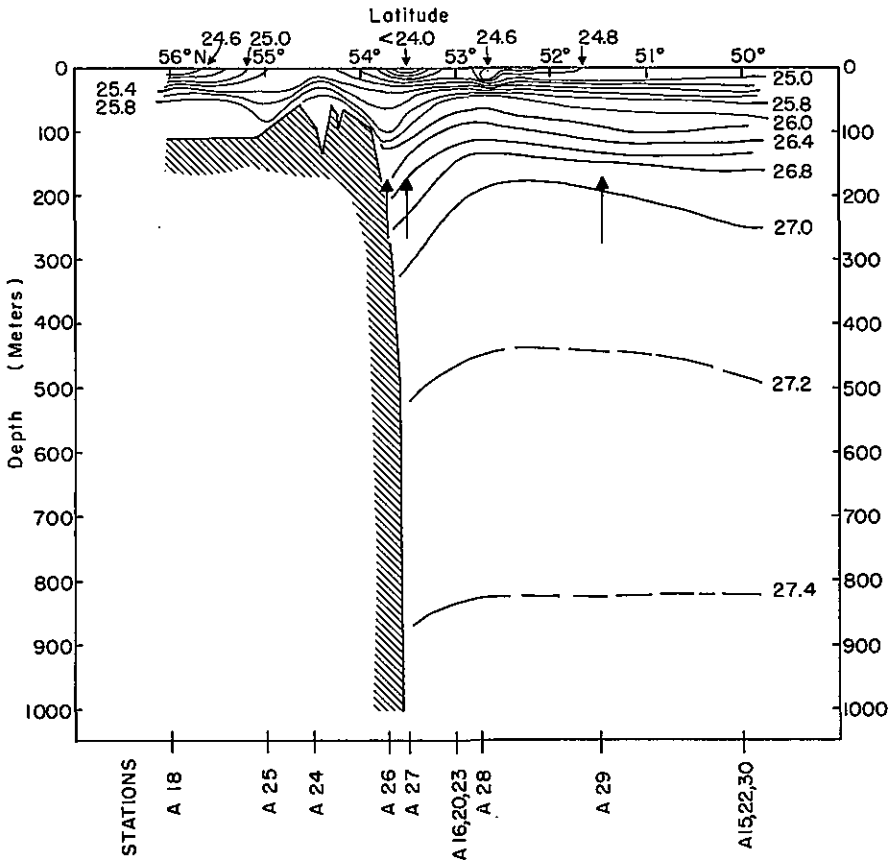

Figure 29.--Vertical distribution of sigma-t along 165°W. longitude, July-August, 1957. Large arrows indicate depths of Nansen bottle casts not reaching 1000 meters (south of 54 N.)

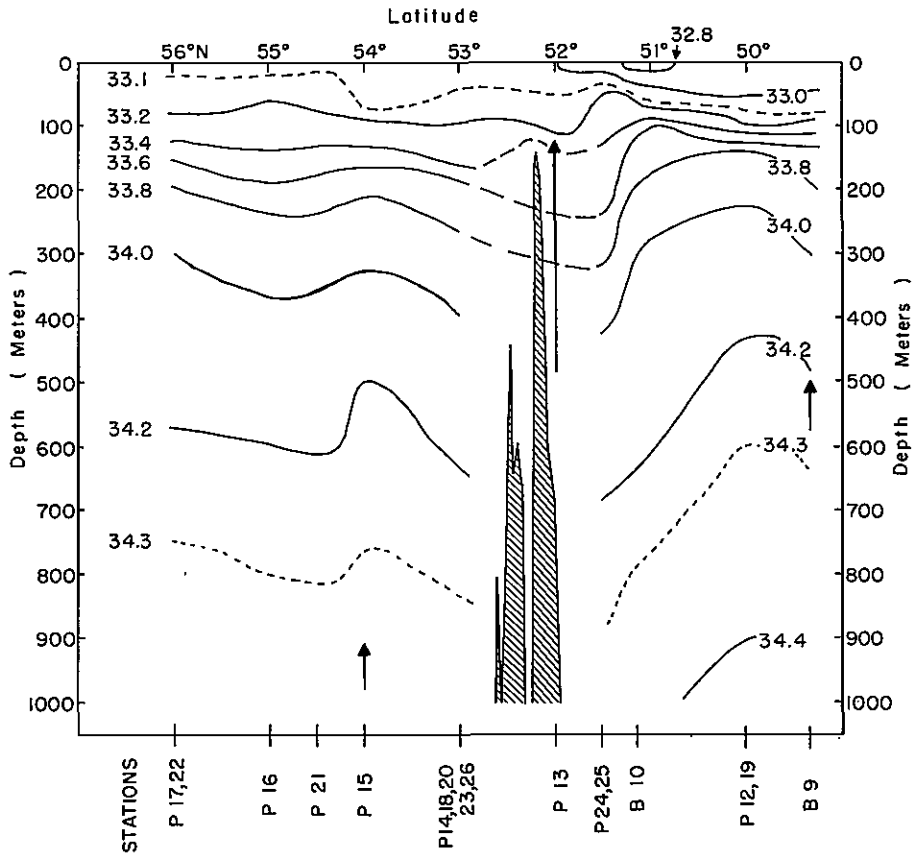

Figure 30.--Vertical distribution of salinity (°/oo) along 175°E. longitude, July-August, 1957. Large arrows indicate depth of Nansen bottle cast not reaching 1000 meters.

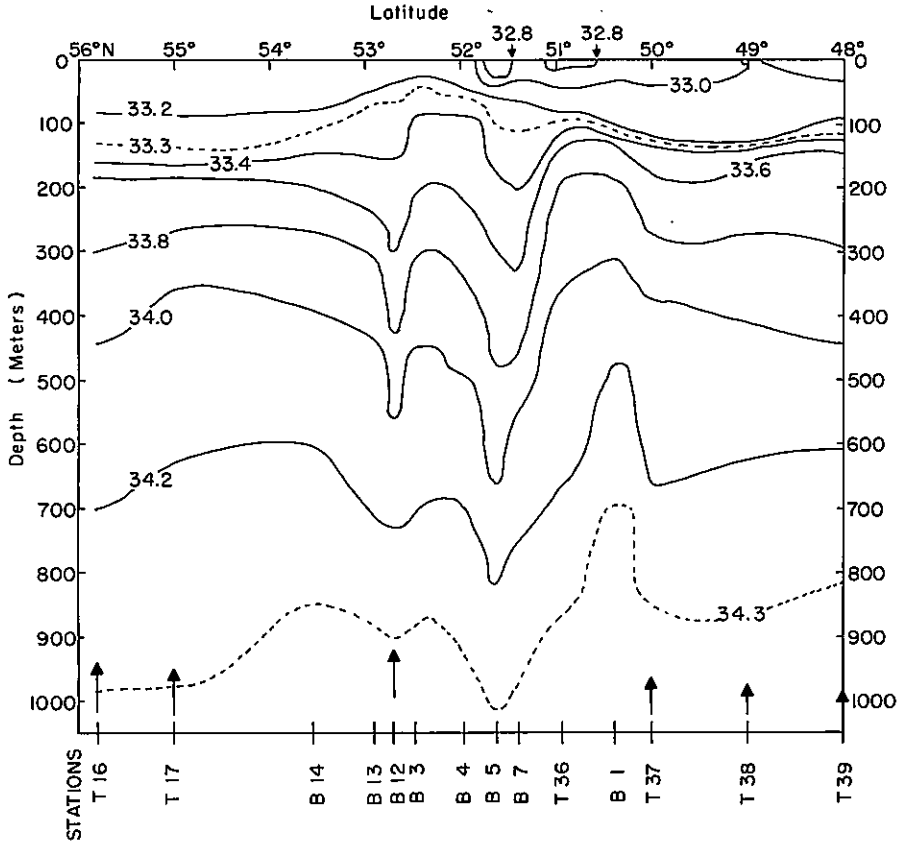

Figure 31.--Vertical distribution of salinity (°/oo) along 179°W. longitude, July-August, 1957. Large arrows indicate depth of Nansen bottle cast not reaching 1000 meters.

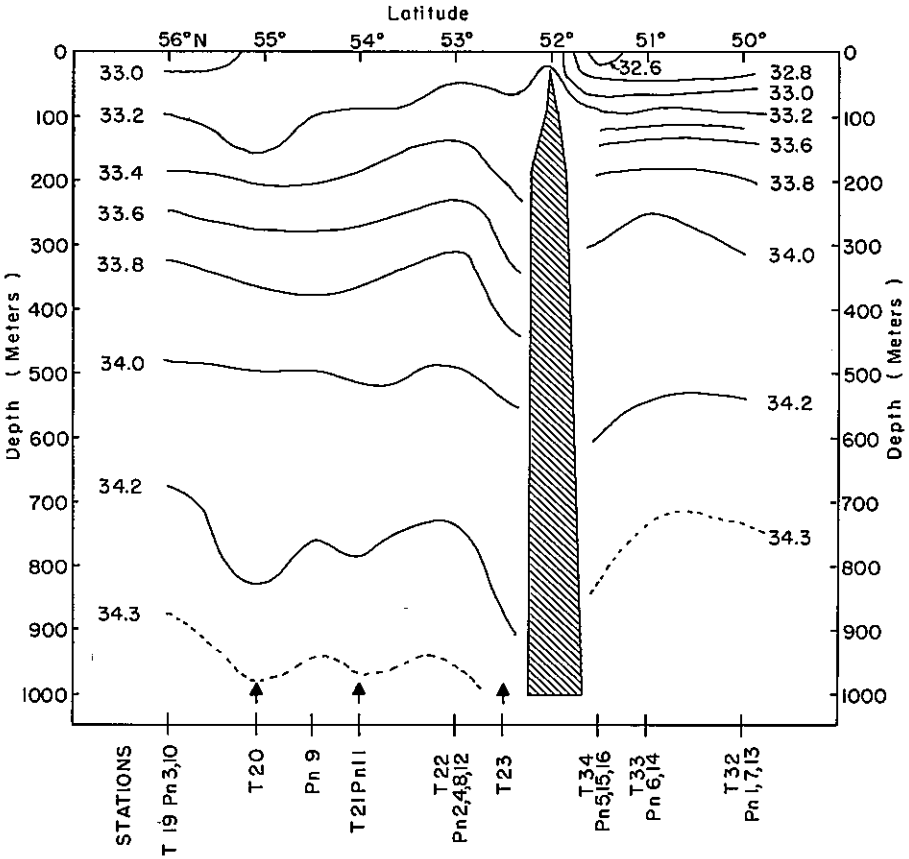

Figure 32.--Vertical distribution of salinity (°/oo) along 175°W. longitude, July-August, 1957. Large arrows indicate depth of Nansen bottle cast not reaching 1000 meters.

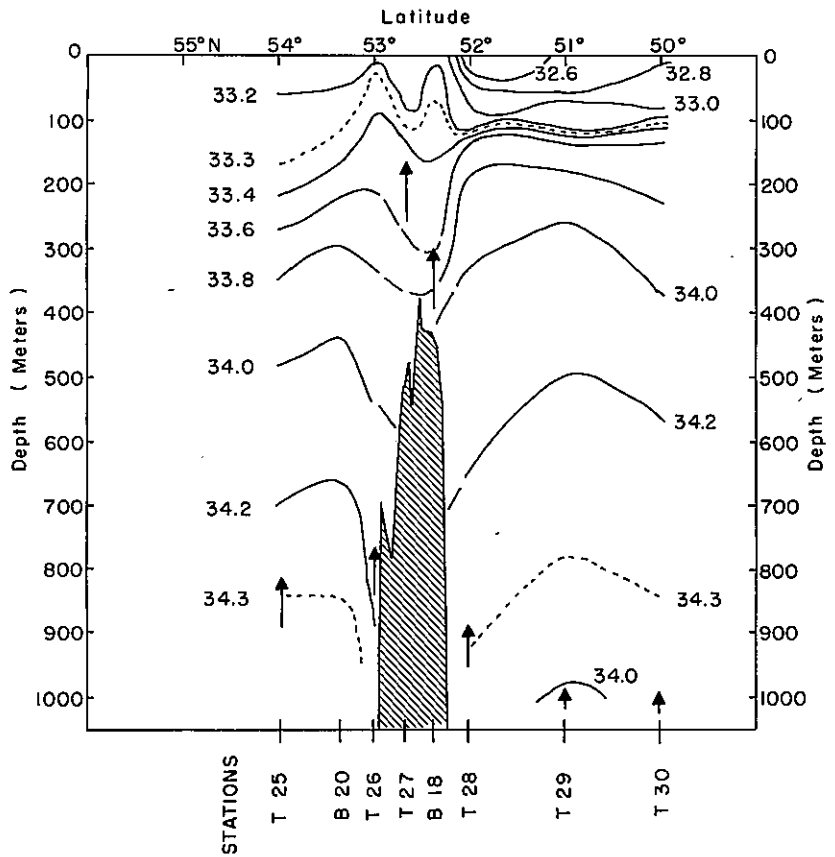

Figure 33.--Vertical distribution of salinity (°/oo) along 171°W. longitude, July-August, 1957. Large arrows indicate depth of Nansen bottle cast not reaching 1000 meters.

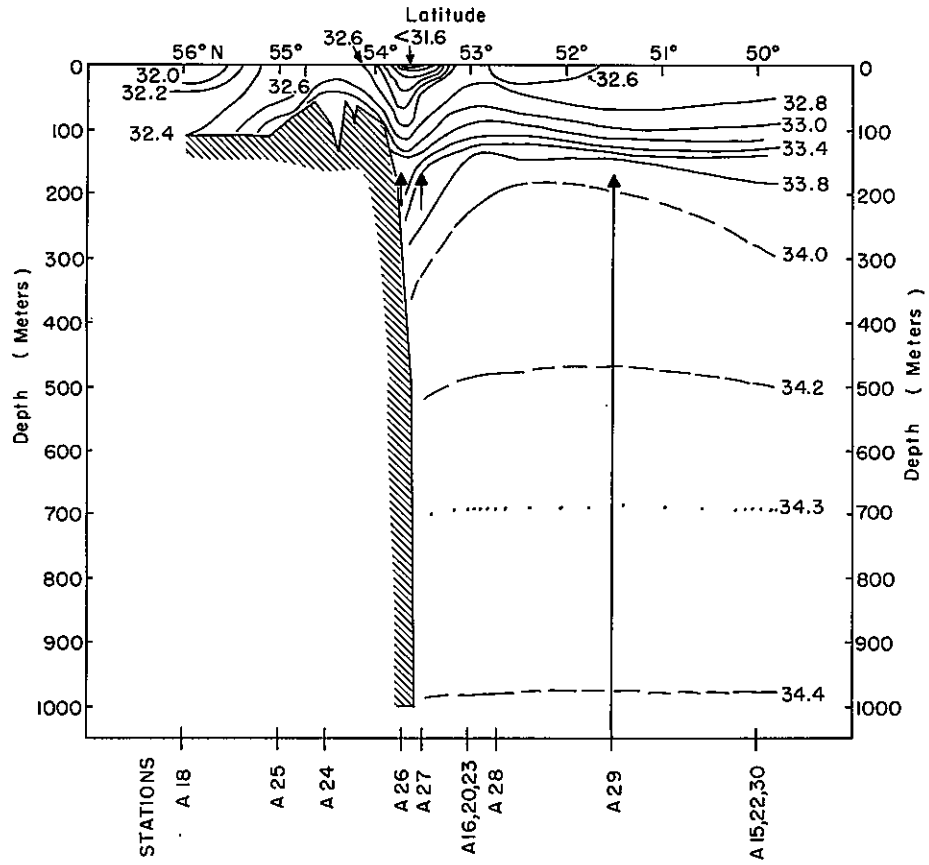

Figure 34.--Vertical distribution of salinity (°/oo) along 165°W. longitude, July-August, 1957. Large arrows indicate depth of Nansen bottle cast not reaching 1000 meters.

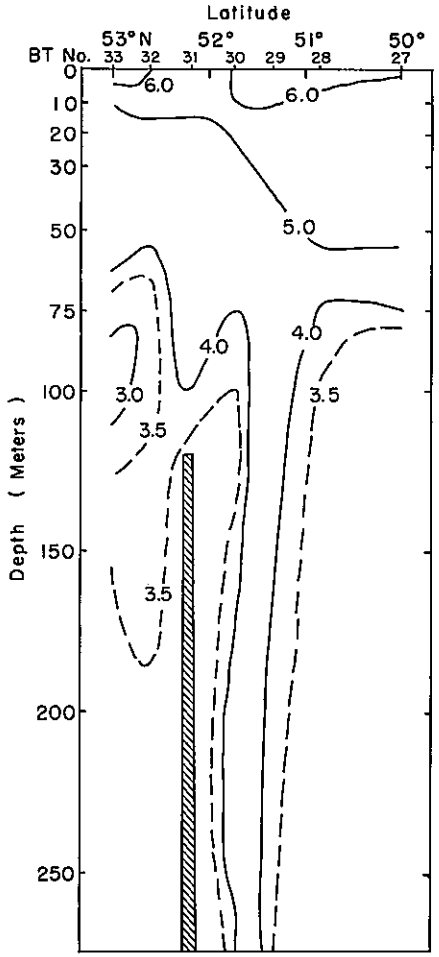

Figure 35.--Bathythermograph (M, °C.) section along 175 E. longitude, MV Pioneer, June 12-14, 1957. BT 27-33.

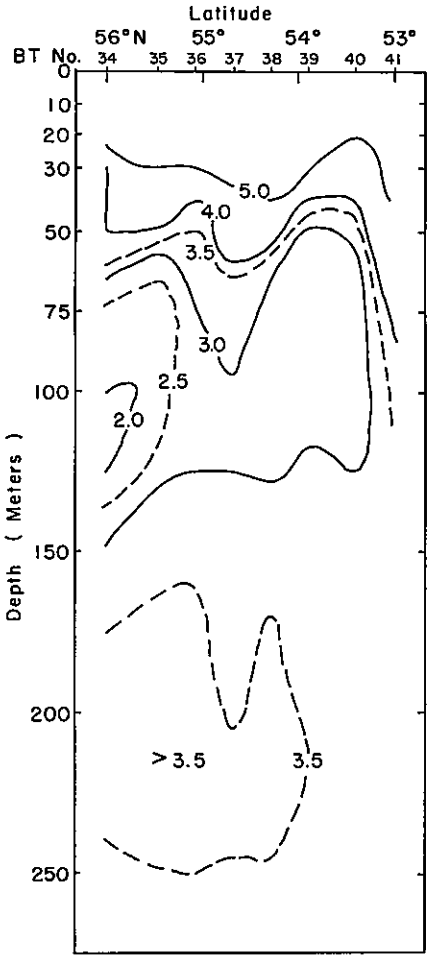

Figure 36.--Bathythermograph (M, °C.) section along 175 E. longitude, MV Pioneer, June 17-20, 1957. BT 34-41.

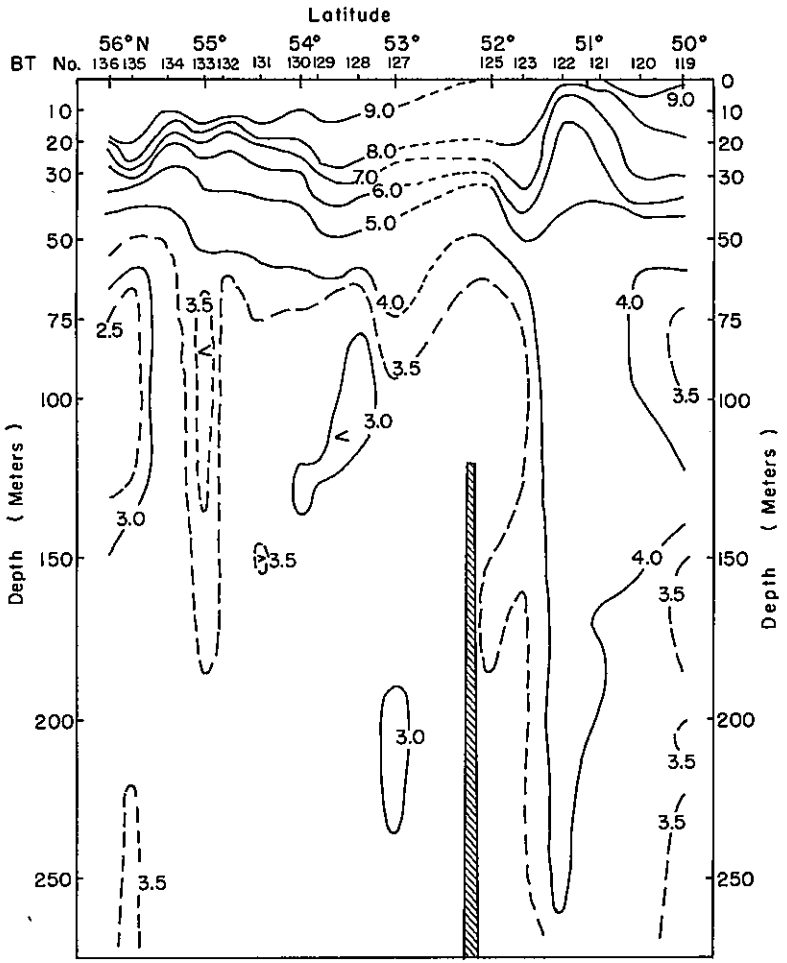

Figure 37.--Bathythermograph (M, °C.) section along 175 E. longitude, MV Pioneer, July 22-27, 1957. BT 119-136.

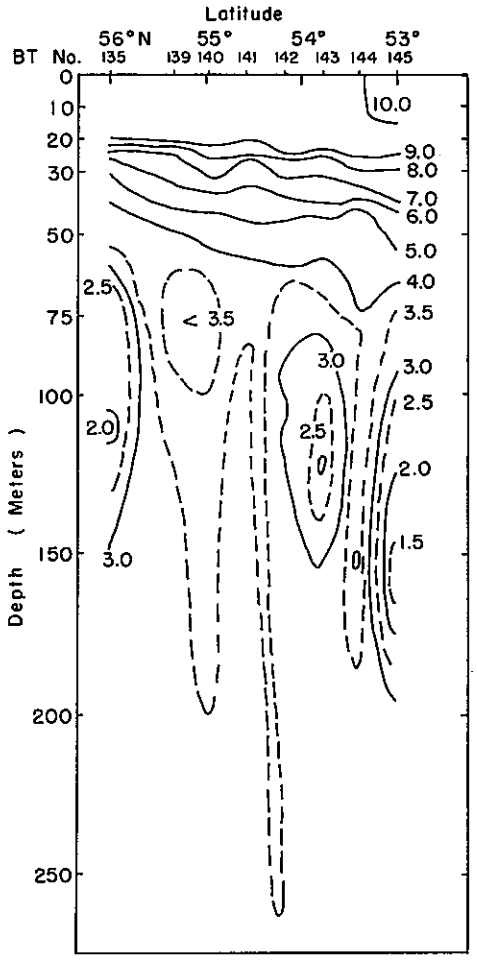

Figure 38.--Bathythermograph (M, °C.) section along 175°E. longitude, MV Pioneer, July 28-29, 1957. BT 138-145.

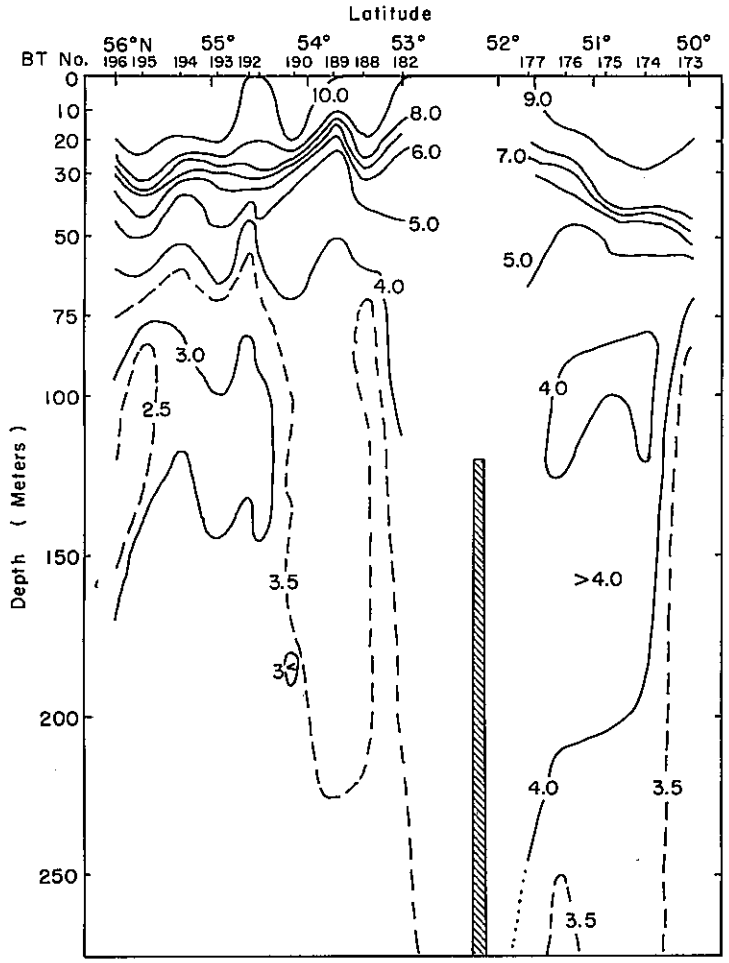

Figure 39.--Bathythermograph (M, °C.) section along 175°E. longitude, MV Pioneer, August 9-14, 1957. BT 173-196.

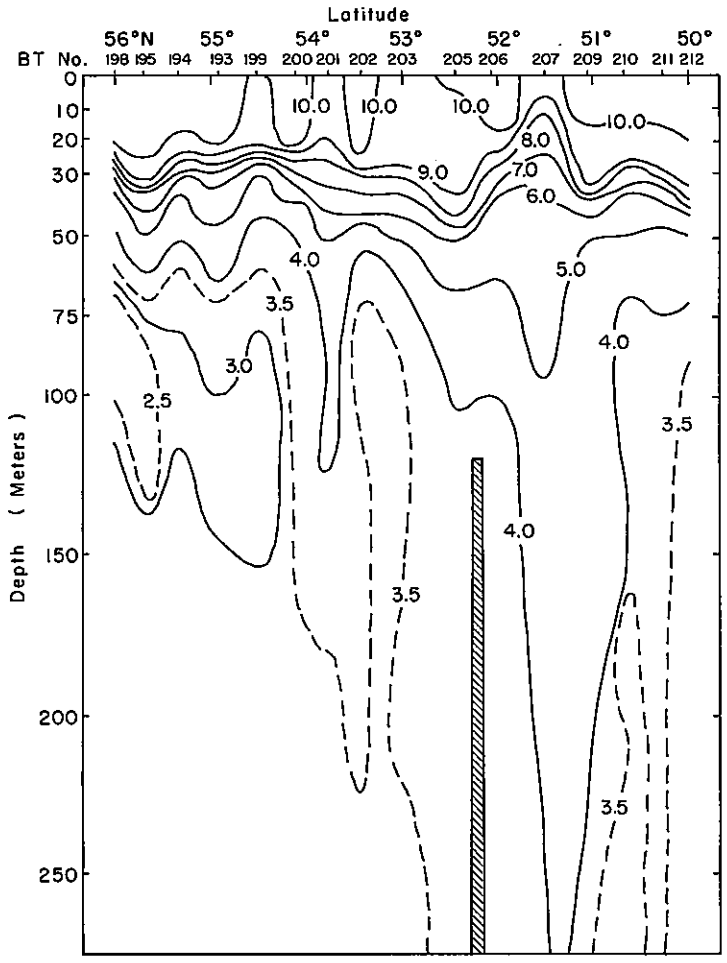

Figure 40.--Bathythermograph (M, °C.) section along 175°E. longitude, MV Pioneer, August 14-20, 1957. BT 193-212.

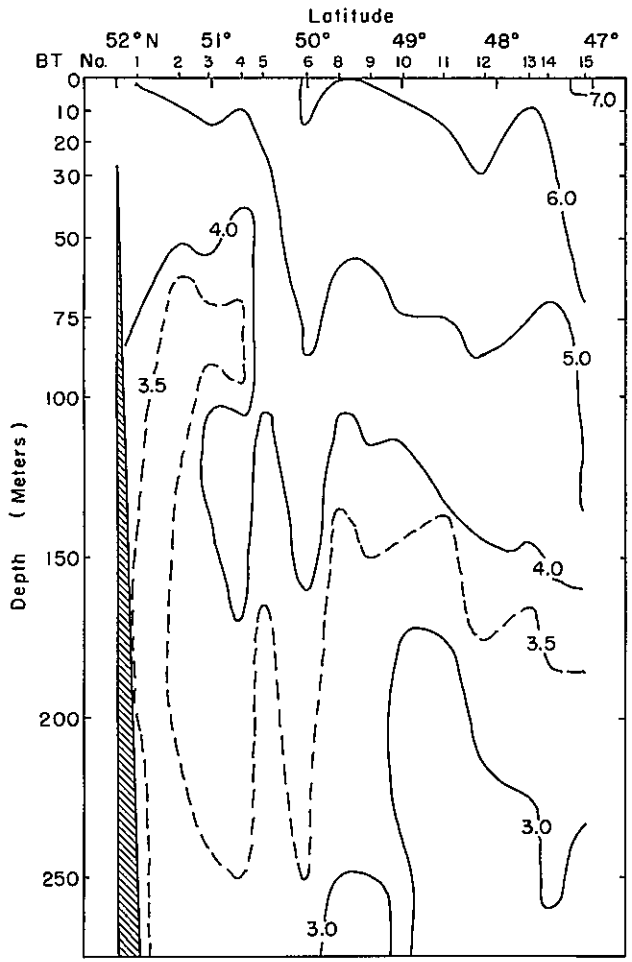

Figure 41.--Bathythermograph (M, °C.) section along 175°W. longitude, MV Attu, May 27 - June 1, 1957. BT 1-15.

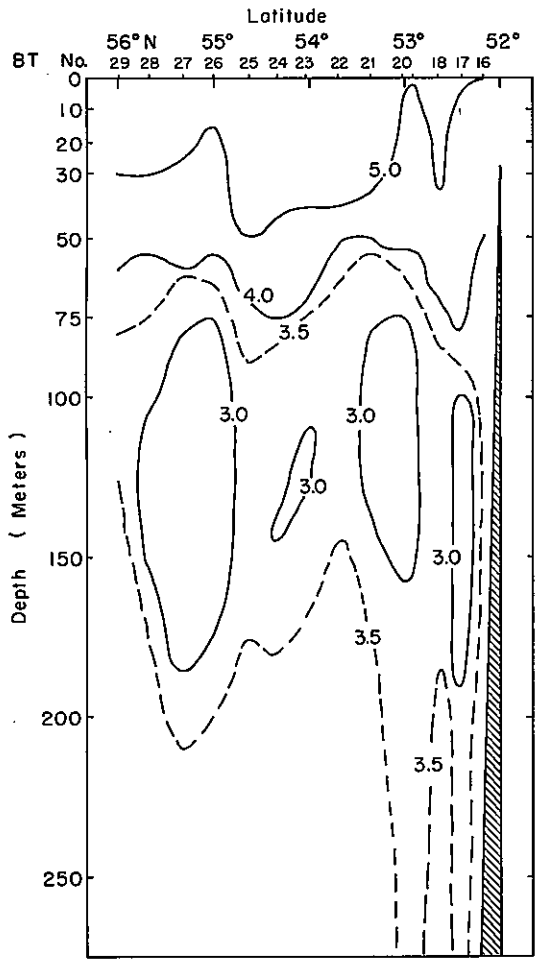

Figure 42.--Bathythermograph (M, °C.) section along 175°W. longitude, MV Attu, June 7-8 (BT 16-20), June 14-15 (BT 21-29), 1957

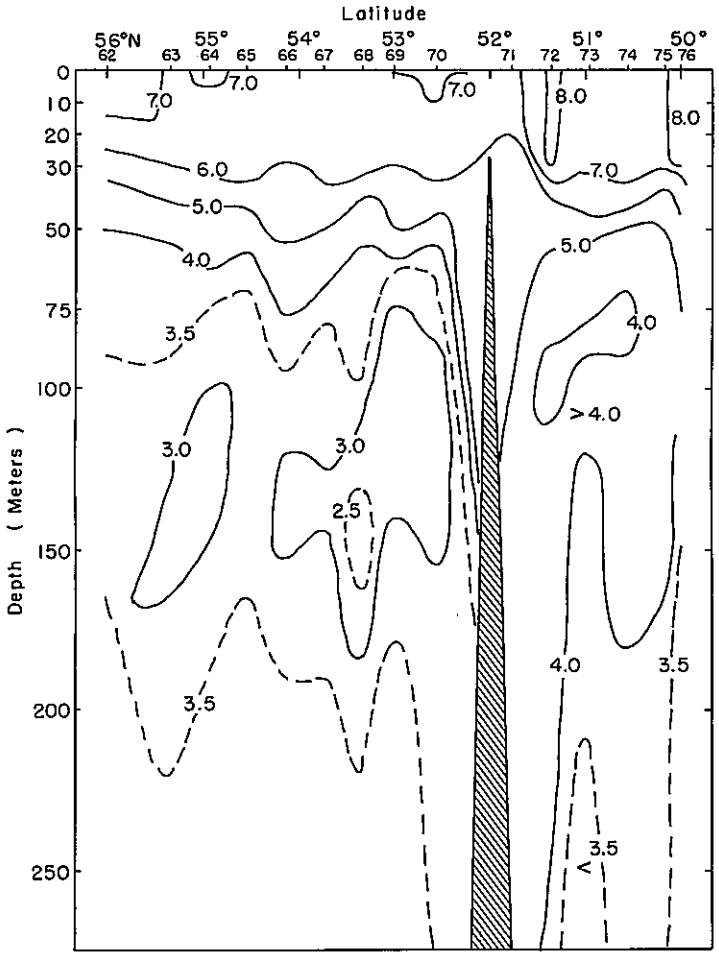

Figure 43.--Bathythermograph (M, °C.) section along 175°W. longitude, MV Pioneer, June 30-July 5, 1957. BT 62-76.

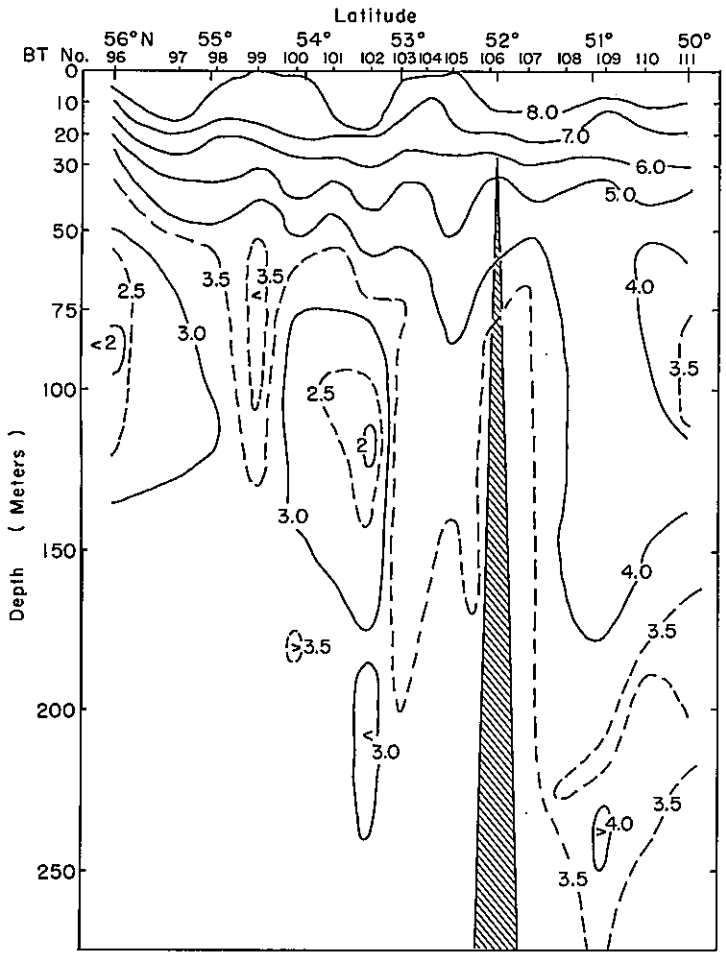

Figure 44.--Bathythermograph (M, °C.) section along 175°W. longitude, MV Pioneer, July 16-20, 1957. BT 96-111.

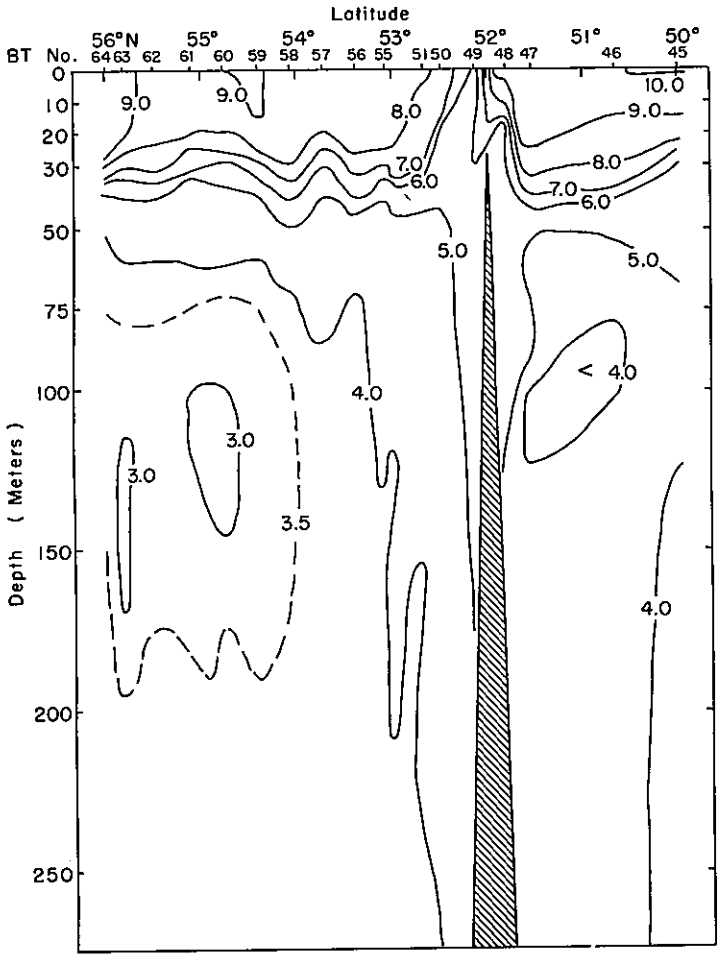

Figure 45.--Bathythermograph (M, °C.) section along 175°W. longitude, MV Paragon, July 22-27, 1957. BT 45-64.

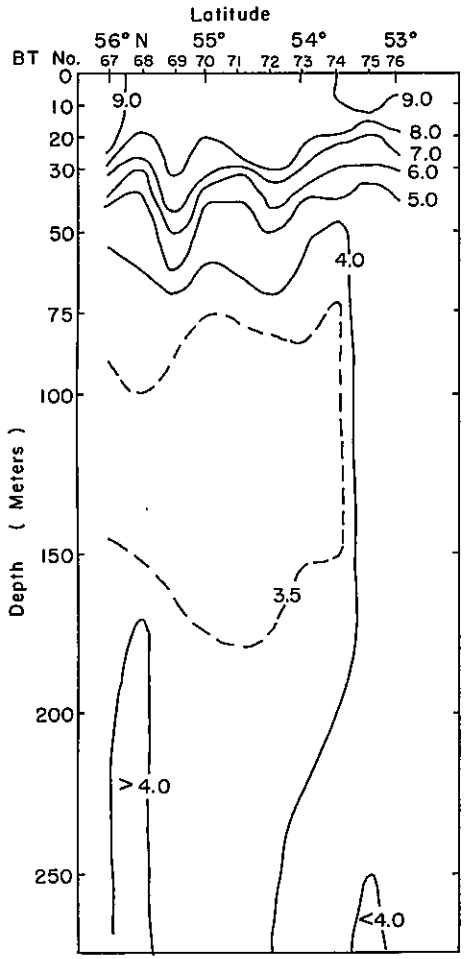

Figure 46.--Bathythermograph (M, °C.) section along 175°W. longitude, MV Paragon, July 28-30, 1957. BT 67-76.

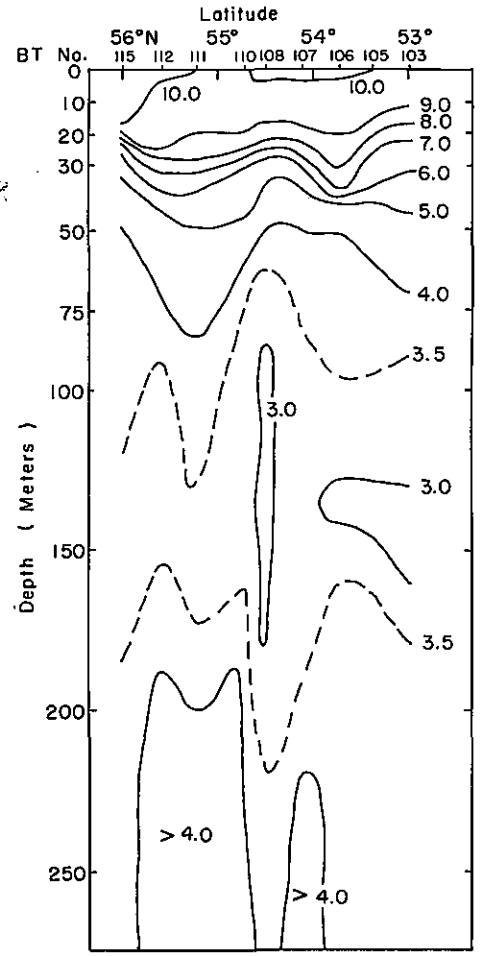

Figure 47.--Bathythermograph (M, °C.) section along 175°W. longitude, MV Paragon, August 12-15, 1957. BT 103-115.

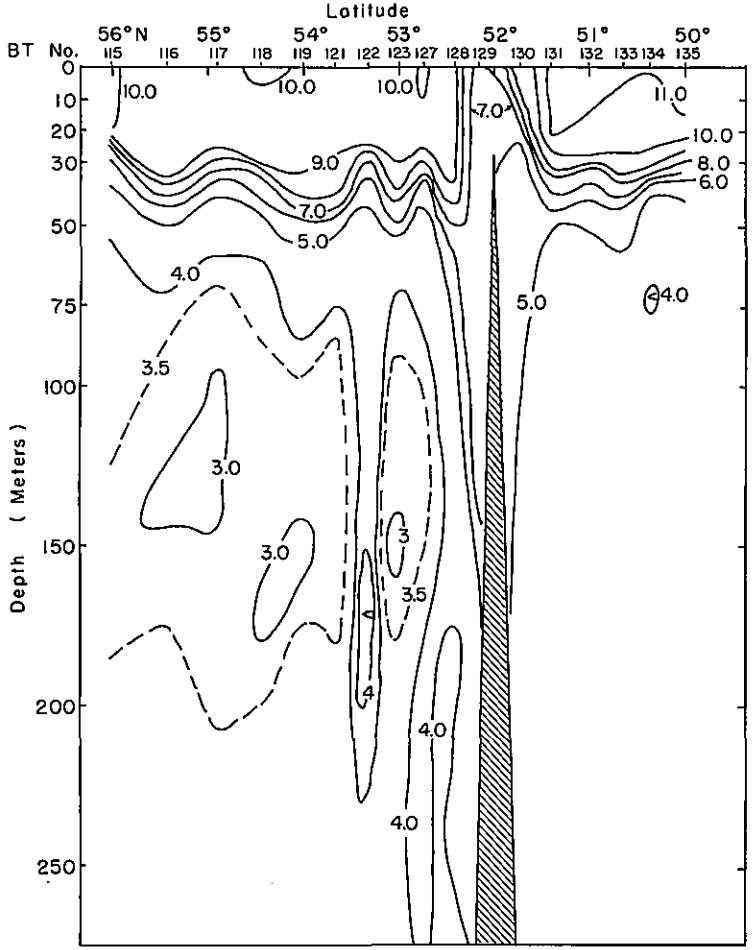

Figure 48.--Bathythermograph (M, °C.) section along 175°W. longitude, MV Paragon, August 15-20, 1957. BT 115-135.

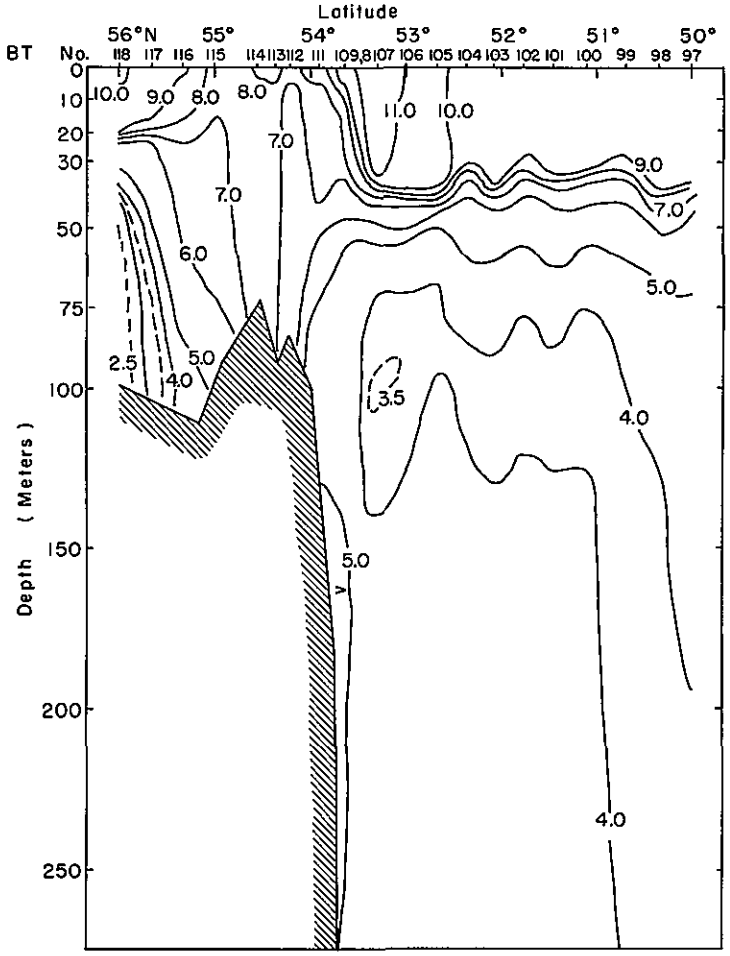

Figure 49.--Bathythermograph (M, °C.) section along 165°W. longitude, MV Attu, July 22-27, 1957. BT 97-118.

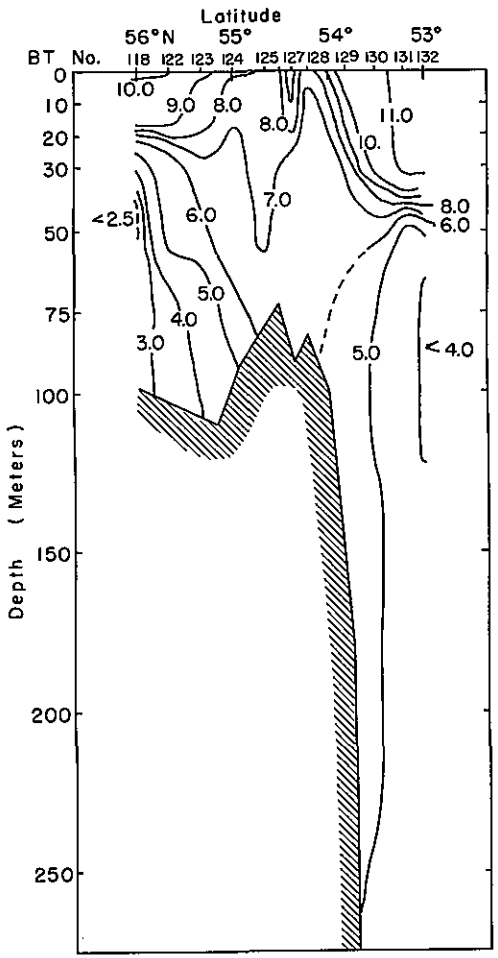

Figure 50.--Bathythermograph (M, °C.) section along 165°W. longitude, MV Attu, July 27-30, 1957. BT 118-132.

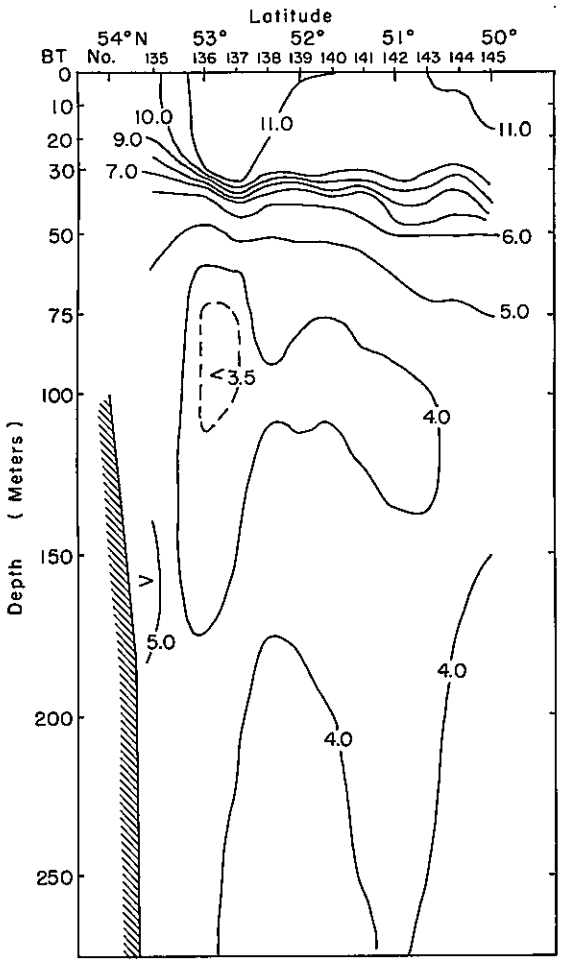

Figure 51.--Bathythermograph (M, °C.) section along 165°W. longitude, MV Attu, August 7-9, 1957. BT 135-145.

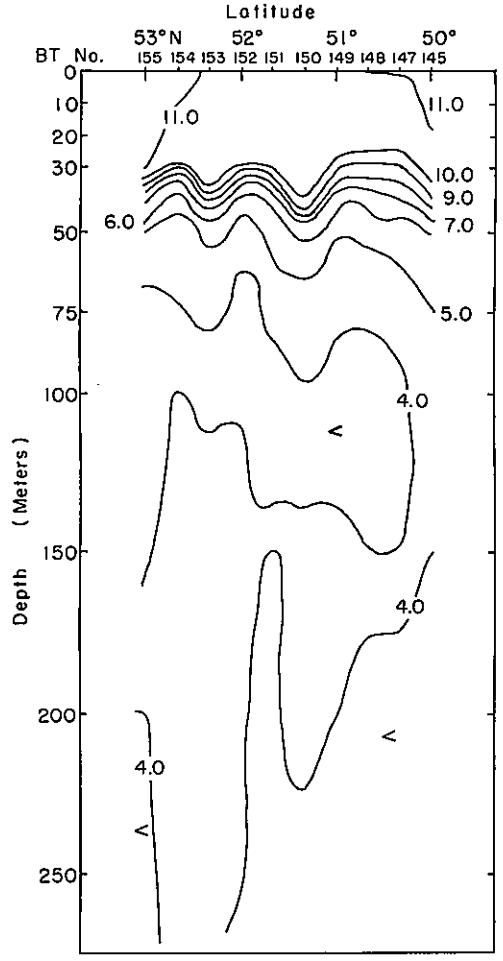

Figure 52.--Bathythermograph (M, °C.) section along 165°W. longitude, MV Attu, August 9-15, 1957. BT 145-155.

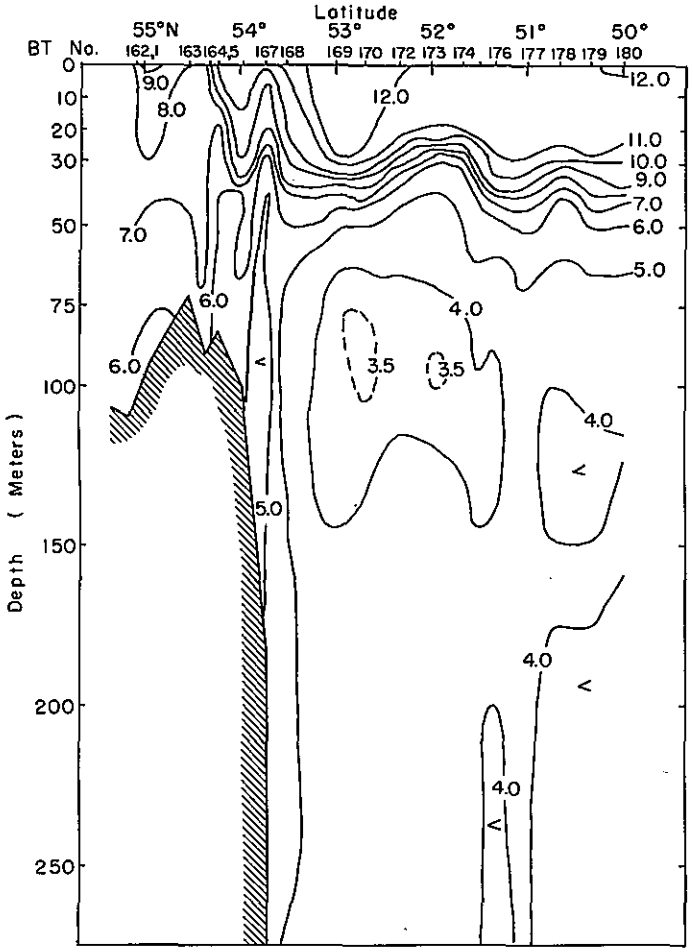

Figure 53.--Bathythermograph (M, °C.) section along 165°W. longitude, MV Attu, August 15-20, 1957. BT 161-180.

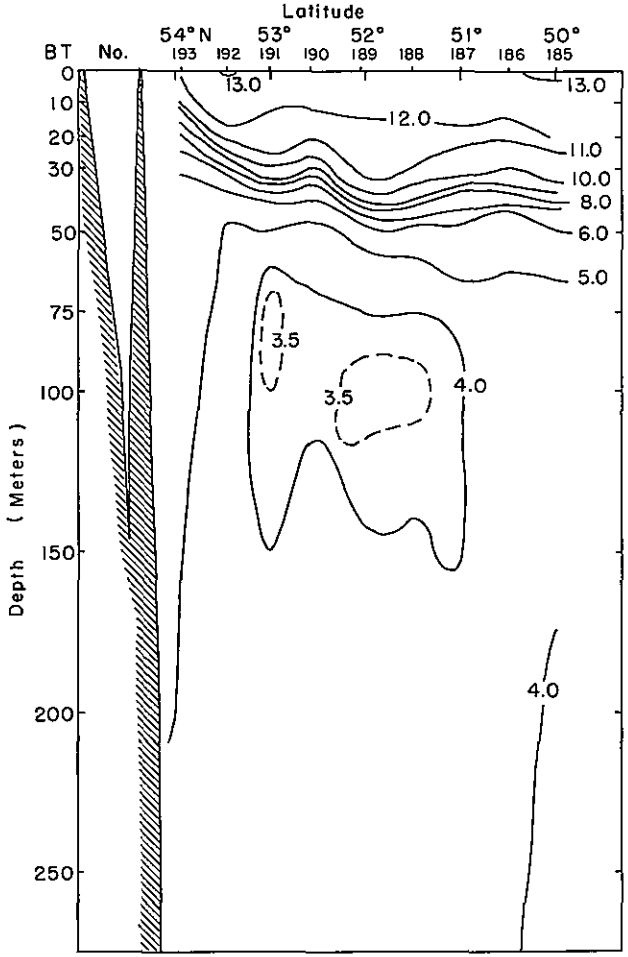

Figure 54.--Bathythermograph (M, °C.) section along 162° 30'W. longitude, MV Attu, August 22-23, 1957. BT 185-193.

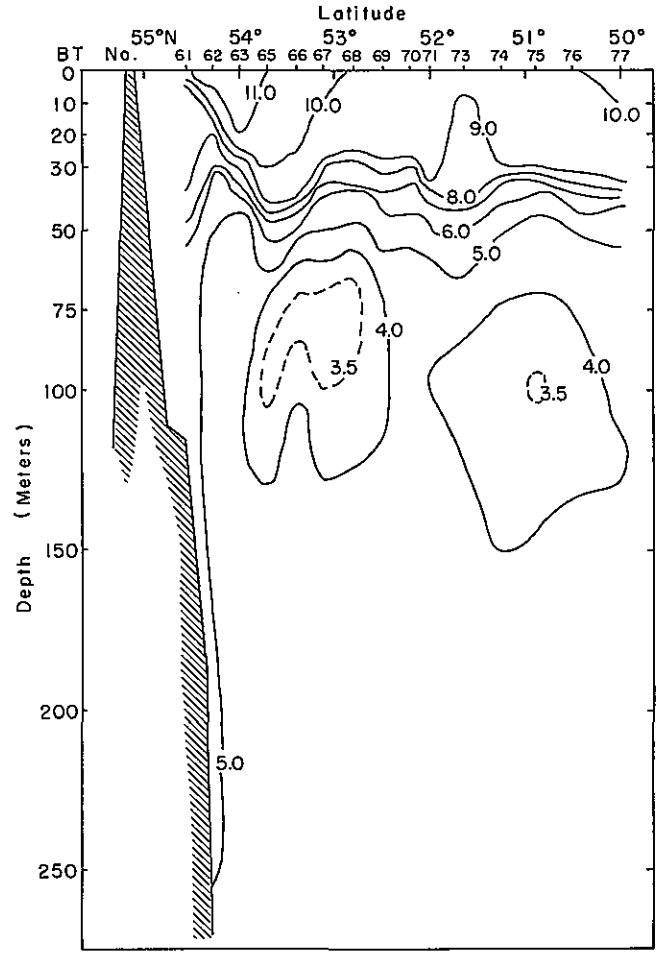

Figure 55.--Bathythermograph (M, °C.) section along 160°W. longitude, MV Attu, July 14-19, 1957. BT 61-77.

GPO 994762